CSIAM Trans. Life Sci.
doi: 10.4208/csiam-ls.SO-2025-0005

Vol. **x**, No. x, pp. 1-39
xx 2025

Co-Evolution of Behavior Change and Infectious Disease Transmission Dynamics: A Modelling Review

Tangjuan Li[1] and Yanni Xiao[2,*]

[1] *School of Mathematical Sciences, Jiangsu University, Zhenjiang 212013, China.*
[2] *School of Mathematics and Statistics, Xi'an Jiaotong University, Xi'an 710049, China.*

Received 1 April 2025; Accepted 24 August 2025

Abstract. During infectious disease outbreaks, the dissemination of information and the dynamic adjustment of intervention strategies trigger psychological and behavioral changes among individuals, which significantly influence disease transmission. Mathematical models have played a crucial role in analyzing the interplay between behavioral changes and disease spread. In this review, we revisit research studies that model behavioral changes during epidemics and classify the literature based on different modeling approaches. Specifically, we categorize these models into three main types: (1) modifying the incidence function to incorporate behavior-driven changes, including a novel approach that utilizes neural networks to describe the incidence rate; (2) introducing additional compartments to represent subpopulations with different behaviors; and (3) employing game-theoretic modeling to study the interactions between infectious disease dynamics and behavioral changes. In the game-theoretic framework, we also examine how key epidemiological metrics – such as the peak size and peak time of the first wave, as well as the final epidemic size – are affected when behavioral changes are incorporated into the classic SIR model. For each category, we introduce the classical modeling frameworks and their extensions, analyzing their advantages and limitations. Finally, we summarize the key findings and outline several promising directions for future research.

AMS subject classifications: 92D30, 92B05

Key words: Epidemic model, behavior change, game theory, co-evolution.

1 Introduction

Infectious diseases pose significant threats to individual health, while also exerting profound impacts on social stability and economic prosperity. Tracing back to the 14th cen-

*Corresponding author. *Email address:* yxiao@mail.xjtu.edu.cn (Y. Xiao)

tury, the Black Death ravaged Europe, claiming over 20 million lives – approximately one-third of the continent's total population [54]. Throughout history, pandemics such as the Spanish flu, HIV/AIDS, and Ebola have resulted in countless fatalities, political instability, and substantial financial and psychosocial burdens [57]. Most recently, the COVID-19 pandemic caused more than 10 million deaths globally [52], triggered massive economic expenditures, surged unemployment rates, and severely disrupted social stability [9]. Consequently, understanding the various factors influencing the spread of infectious diseases, analyzing the dynamics under these factors, and identifying effective intervention strategies are of critical importance.

The impact of infectious diseases on society is profound and far-reaching, extending beyond public policy and control measures to influence individual behavior and psychological responses. For instance, during the 2009 H1N1 influenza pandemic, self-protective measures, including increased handwashing, covering one's mouth and nose while coughing, and minimizing contact with others, significantly reduced infection risks [74]. Home isolation has proven to be an effective method for reducing disease transmission and maintaining social distancing. However, severe influenza pandemics necessitate stricter social distancing measures [22]. Recently, several studies have investigated behavioral changes as effective strategies to mitigate the spread of COVID-19. Kucharski *et al.* [34] demonstrated that combining self-isolation, contact tracing, and moderate social distancing could effectively control the transmission of COVID-19. Buonomo and Della Marca [12] highlighted the decisive role of strict adherence to preventive measures in significantly reducing both mortality and new infections. Tang *et al.* [77] pointed out that, to prevent subsequent pandemic waves, sustained and effective behavioral changes are critical, particularly during the early stages of vaccine rollout. During outbreaks, individuals adjust their behavior based on perceived infection risks, and these behavioral decisions, in turn, influence disease transmission dynamics. Therefore, analyzing the interplay between behavioral changes and disease transmission, and identifying key factors driving pandemic spread, are essential for understanding the dynamical patterns of infectious diseases and developing effective control strategies. Behavioral shifts may arise from voluntary or passive decisions, or from the cost-benefit trade-offs associated with specific actions [24, 78]. This heterogeneity in behavior presents significant challenges in accurately quantifying behavioral responses and understanding the complex interactions between behavior change and disease transmission dynamics.

A variety of mathematical models have been developed to explore human behavior dynamics, including models of panic-driven escape [27], pedestrian path choice [28], and traffic congestion phenomena [88]. In the context of behavior change during epidemic outbreaks, one of the most straightforward approaches is to evaluate the effectiveness of public health interventions, such as assessing the impact of school closures on disease spread [10]. Furthermore, the influence of behavioral evolution on transmission can be described by altering individuals' epidemiological states during transmission, such as the transition from susceptible to immune status following vaccination, or by modifying the infection or recovery rates [24]. Numerous reviews have explored the impact of hu-

man behavior on the spread of infectious diseases. For example, Funk *et al.* [24] provide a comprehensive review of models categorized by the type and source of information influencing individual behavior, as well as the behavioral effects assumed in these models. Verelst *et al.* [82] present a systematic review of behavioral change models for infectious disease transmission from 2010 to 2015. Weston *et al.* [87] focus on original research articles featuring infectious disease models with human-to-human transmission, where individuals' self-protective health behaviors vary endogenously. Hidano *et al.* [29] give a review about modeling dynamic human behavioral changes in animal disease models. Chang *et al.* [14] review game-theoretic models of infectious disease dynamics and intervention strategies. Sooknanan *et al.* [72,73] examine major approaches for incorporating behavior changes driven by online media into compartmental models.

In this review, we specifically focus on the interaction between disease transmission and behavioral changes at the population level. We begin by presenting three general disease transmission models that incorporate behavioral changes, followed by a detailed review of the relevant literature, organized according to different modeling approaches. For each category, we first introduce a classical modeling framework, then discuss a series of extended models, highlighting their advantages and limitations. Additionally, we explore a novel and promising approach that integrates machine learning with traditional ODE-based disease models to examine the interplay between behavioral changes and disease transmission. To better understand the impact of modeling approaches that capture transitions between behavioral subgroups through game theory, we examine key epidemiological outcomes, including peak size, peak time of the first wave, and final epidemic size, based on the classical SIR model. Finally, we conclude with a summary and provide an outlook on future research directions.

2 General framework of models with behavioral change

Mathematically, behavioral changes can be incorporated into infectious disease models by adjusting or refining the incidence rate, for instance, by introducing a severity-dependent decreasing function that reduces infection or contact rates as the epidemic progresses. For a general system, consider the following equation:

$$\frac{dI(t)}{dt} = \lambda(t,S,I,\psi) - \gamma I(t), \tag{2.1}$$

where $I(t)$ (or $S(t)$) represents the number or proportion of infectious (susceptible) individuals, γ is the removal rate of $I(t)$, $\lambda(t,S,I,\psi)$ represents the incidence rate, ψ denotes parameters or functions related to behavioral changes, such as prevalence-dependent contact rate, surveillance rate, or isolation rate. Note that $\lambda(t,S,I,\psi)$ can also be modeled using neural networks, leading to a neural differential equation.

Another approach in modeling is to describe the dynamic evolution of different behavioral subgroups. To do so, a population (say infectious individuals) may be divided

into, say, two subgroups that adopt behavior 1 (say normal behavior) and behavior 2 (say, altered behaviors) according to types of behavior. Then we have the following description:

$$\begin{cases} \dfrac{dI_1(t)}{dt} = f_1(t,I,S,\phi_1) - g_1(t,I,S,b) + g_2(t,I,S,b), \\ \dfrac{dI_2(t)}{dt} = f_2(t,I,S,\phi_2) + g_1(t,I,S,b) - g_2(t,I,S,b), \end{cases} \tag{2.2}$$

where I_1 and I_2 represent the proportion or total numbers of infectious individuals in subgroups that adopt behavior 1 and behavior 2, respectively. The functions $f_1(\cdot)$ and $f_2(\cdot)$ describe the disease transmission process for each behavioral group, while $g_1(\cdot)$ and $g_2(\cdot)$ characterize the transitions between two subgroups resulting from behavioral changes. Notably, the transition functions $g_1(\cdot)$ and $g_2(\cdot)$ may depend on disease prevalence, incidence of new infections, or the level of information dissemination. The parameters ϕ_1 and ϕ_2 are related to the disease transmission for each behavioral subgroup, and b denotes a parameter related to behavioral changes.

Moreover, human behavior is shaped by evaluating potential outcomes of different decisions based on cost-benefit analyses. Factors such as past experiences, reactions to others' actions, and shifts in external conditions influence this decision-making process. Game theory offers a comprehensive and intuitive framework to model these dynamics [83]. One simple way to incorporate decision-making processes is by allowing one parameter of the traditional disease model to vary over time, in accordance with game theory principles. Taking vaccination as an example, this can be expressed as follows:

$$\begin{cases} \dfrac{dS}{dt} = \mu p - \beta SI - \mu S, \\ \dfrac{dp}{dt} = p(1-p) f(p,I), \end{cases} \tag{2.3}$$

where p represents the time-varying fraction of individuals who vaccinate at birth, with p being determined by game theory. The other approach assumes that the transitions between different behavioral subgroups follow game-theoretic principles. Similar to the system in Eq. (2.2), the transitions between I_1 and I_2 are governed by game theory, as illustrated by the following expressions:

$$g_1(I_1,I_2,k,m) = kI_1I_2P_2(I,m), \quad g_2(I_1,I_2,k,m) = kI_1I_2P_1(I,m), \tag{2.4}$$

where k and m are constant parameters, and $P_1(I,m)$ and $P_2(I,m)$ represent the pay-off functions for behaviors 1 and 2, respectively. These pay-off functions are influenced by the prevalence I, with one underlying implication being that individuals tend to adopt the behavior that offers the higher payoff, reflecting rational decision-making in their responses to the epidemic.

In the upcoming sections, we will provide a comprehensive review of the relevant literature, organized by modeling categories in order. Each category begins with an introduction to a classical modeling approach, followed by a discussion of various extended models, along with an evaluation of their strengths and weaknesses.

3 Revising the incidence function to incorporate behavior-driven changes

During an epidemic outbreak, the intensity of behavioral changes is often influenced by the current level of disease prevalence. Timely information about a disease, including updates disseminated through media and social networks, has been demonstrated to play a critical role in mitigating its spread [47]. In general, the more severe the outbreak, the greater the number of individuals adopting behavioral changes or the intensity of those changes, which can be reflected by modifying the incidence rate.

3.1 Models with rational-type nonlinear incidence rate

One common approach to modelling behavior change is to formulate a general incidence function, which could be a nonlinear rational function, to represent the comprehensive effect of behavior changes. Let us take an SIRS-type model as an example to illustrate

$$\begin{cases} \dfrac{dS}{dt} = \Lambda - dS - \lambda(S,I) + \delta R, \\ \dfrac{dI}{dt} = \lambda(S,I) - (d+\gamma)I, \\ \dfrac{dR}{dt} = \gamma I - (d+\delta)R, \end{cases} \tag{3.1}$$

where S, I and R represent the number of susceptible, infected, and recovered individuals, respectively, and $\lambda(S,I)$ represents the incidence rate. In particular, Liu *et al.* [43] considered a generalized incidence rate of the form $\lambda(S,I) = \beta I^p S^q$, where $\beta, p, q > 0$. They found that both saddle-node and Hopf bifurcations may occur under certain conditions. Their work also included an alternative form of the incidence rate $\lambda(S,I) = kS^q I^p/(1+mI^{p-1})$, with $m>0$ and $p>1$, and analyzed the conditions under which Hopf bifurcations can arise in this setting. Subsequently, Liu *et al.* [42] showed that a wide range of epidemiological models, including SIS, SIR, SEIS, SEIR and SEIRS, incorporating $\beta I^p S^q$ as a nonlinear incidence rate, exhibit a much richer set of dynamical behaviors than those based on the standard bilinear incidence. And for the SEIRS model, periodic solutions may arise through Hopf bifurcation at certain critical parameter values. Xiao *et al.* [89] defined the incidence rate as $\lambda(S,I) = kIS/(1+\alpha I^2)$ and calculated the basic reproduction number, R_0. They found that the disease-free equilibrium is globally asymptotically stable when $R_0 < 1$. Conversely, when $R_0 > 1$, the system has a unique endemic equilibrium that is globally asymptotically stable. Furthermore, R_0 is independent of the parameter α, indicating that behavioral changes do not affect the dynamical behavior of the model. Building on this framework, various forms of nonlinear functions have been introduced to further refine the incidence rate [44–46, 64, 80, 85, 94]. These are expressed as $\lambda(S,I) = \beta(I)SI$, where $\beta(I)$ is a nonlinear saturation function of I. The main results associated with these models are summarized in Table 1. This modeling approach

Table 1: Revising the incidence function using saturation functions.

Reference, basic model	Incidence function	Main conclusion
[64] SIRS	$\beta(I)SI$ with $\beta(I)=\frac{\beta I}{1+\alpha I^2}$.	The system undergoes Bogdanov-Takens bifurcations as parameters vary.
[85] SIRS	$\frac{\lambda IS}{f(I)}$ with $f(0)>0, f'(I)>0$ and $\left(\frac{I}{f(I)}\right)'=\begin{cases}>0, & 0<I<\xi,\\ <0, & I>\xi.\end{cases}$	The system converges to a unique endemic equilibrium when $R_0>1$.
[44] SIRS	$\beta(I)SI$ with $\beta(I)=\beta_1-\beta_2\frac{I}{m+I}$, where β_1 and $\beta(I)$ denote the contact rates before and after behavioral change, respectively.	When $R_0>1$, the system exists a unique endemic equilibrium, which is LAS. On a special case, the endemic equilibrium is GAS.
[94] SIRS	$\beta(I)SI$ with $\beta(I)=\beta_1-\beta_2\frac{I(t-\tau)}{m+I(t-\tau)}$.	The system exhibits Hopf bifurcation at the endemic equilibrium when τ pass through some thresholds.
[80] SIVRS	The incidence rates between S and I, and V and I, are given by $\beta_S(I)SI$ and $(1-r)\beta_V(I)SI$, respectively, where $\beta_S(I)=\beta_1-\beta_2\frac{I}{m+I}$ and $\beta_V(I)=\beta_1-\beta_3\frac{I}{m+I}$.	The parameters β_2, β_3, and m, related to behavior change, do not affect R_0 or the global stability of the disease-free equilibrium.
[45,85] SIRS	$\beta(I)SI$ with $\beta(I)=\frac{\beta I}{1+kI+\alpha I^2}$.	The model undergoes saddle-node bifurcation, Bogdanov-Takens bifurcation of codimension two, Hopf bifurcation, and degenerate Hopf bifurcation of codimension two, the saddle node bifurcationof nonhyperbolic periodic orbit and homoclinic bifurcations.
[46] SIRS	$\beta(I)SI$ with $\beta(I)=\frac{\beta}{1+kI+\alpha I^2}$, where $\alpha>0$ and $k>-2\sqrt{\alpha}$.	The model undergoes saddle-node bifurcation, backward bifurcation, Bogdanov-Takens bifurcation of codimension three, Hopf bifurcation, and degenerate Hopf bifurcation of codimension three.

Note: GAS stands for globally asymptotically stable, while LAS stands for locally asymptotically stable.

can also be extended to patch models. For instance, Sun *et al.* [76] investigate an SIS model on two patches, incorporating the reduction in interpersonal contact due to behavior changes in response to the disease. They assume that new infections in patch i are represented by $\beta_i S_i I_i / N_i$, where $\beta_i(I_i) = a_i - b_i f_i(I_i)$ and $f_i'(I_i) > 0$. It is found that when the basic reproduction number $R_0 < 1$, the system has only one disease free equilibrium, which is globally asymptotically stable. When $R_0 > 1$, the system exists a unique globally asymptotically stable endemic equilibrium. These studies focus on theoretical analysis, such as calculating R_0, analyzing the stability of equilibria, and exploring potential bifurcations. It was shown that oscillations may occur when $\beta(I)$ in $\lambda(S,I) = \beta(I)SI$ is non-monotonic.

3.2 Models with incidence rate modified by an exponential function

Another common approach involves introducing exponential functions to modify the incidence rate. For example, Liu *et al.* [41] proposed an SEIH model by incorporating an exponential function negatively correlated with the number of exposed individuals (E), infected individuals (I), and hospitalized individuals (H)

$$\begin{cases} \dfrac{dE}{dt} = -\beta e^{-a_1 E - a_2 I - a_3 H} SI - \theta E, \\ \dfrac{dI}{dt} = \theta E - (d+h)I, \\ \dfrac{dH}{dt} = hI - (d_h + \gamma)H. \end{cases} \tag{3.2}$$

The basic reproduction number for this model was derived as $R_0 = \beta S_0/(d+h)$. When $R_0 < 1$, the disease-free equilibrium is globally asymptotically stable. When $R_0 > 1$, if $a_1 > 0$ and $a_2 = a_3 = 0$, or if $a_2 > 0$ and $a_1 = a_3 = 0$, the endemic equilibrium is locally asymptotically stable. However, when $R_0 > 1$ and $a_3 > 0$ with $a_1 = a_2 = 0$, the system undergoes a Hopf bifurcation. This demonstrates that while behavioral changes do not affect the basic reproduction number of disease transmission, they can induce oscillation in the system, particularly when the number of hospitalized individuals influences behavior changes. Building on this model, additional related variants [20, 66, 69] are summarized in Table 2. Furthermore, considering the intensity of behavioral changes depends not only on the number of cases but also on the rate of change in cases [79, 90, 91], Xiao *et al.* [91] extended (3.2) by introducing an innovative exponential function, $e^{-M(t)}$, where

$$M(t) = \max\left\{0, p_1 I(t) + p_2 \frac{dI(t)}{dt}\right\}.$$

Using the Lambert W function, the model was transformed into a switching system dependent on whether the susceptible population reaches a critical level S_c. Specifically, the transmission probability becomes a piecewise function, where the effects of behavioral

Table 2: Revising the incidence function using exponential functions.

Reference, basic model	Incidence function	Main conclusion
[41] EIH	$\beta e^{-a_1E-a_2I-a_3H}$, where H represents hospitalized individuals.	When $R_0<1$, the disease-free equilibrium is GAS. For $R_0>1$, the endemic equilibrium is LAS if $a_1>0$ and $a_2=a_3=0$, or $a_2>0$ and $a_1=a_3=0$, but undergoes a Hopf bifurcation if $a_3>0$ and $a_1=a_2=0$.
[20] SEIR	$\beta e^{-mI}SI$ (Note: the Logistic growth is included).	The disease-free equilibrium is GAS when $R_0<1$. For $R_0>1$, a unique endemic equilibrium emerges, and the system may undergo a Hopf bifurcation.
[69] SIR	$\beta e^{-mI(t-\tau)}S(t)I(t)$ with time delay τ denotes response time for individuals to the current infection.	The system undergoes Hopf bifurcation as parameter τ varies.
[66] SEQIHRS	$\beta e^{-(m_1I+m_2H)/N}\frac{S(I+\eta H)}{N}$.	The model has a unique endemic equilibrium whenever the effective reproduction number exceeds unity and the endemic equilibrium is LAS.
[91] SIR	$\beta_0 e^{-M(t)}SI$ with $M(t)=\max\left\{0,p_1I(t)+p_2\frac{dI(t)}{dt}\right\}$.	The proposed model was then converted into a switching system, where the transmission probability is given by $\beta=e^{-\epsilon M_1(t)}\beta_0$ with $\epsilon=\begin{cases}0, & S-S_c\le 0,\\ 1, & S-S_c>0.\end{cases}$ and S_c is a constant.
[79] SIHR	$\beta e^{-M(t)}\frac{I+\varepsilon H}{N}S$ with $M(t)=\max\left\{0,aI(t)+b\frac{dI(t)}{dt}\right\}$.	Numerical simulations demonstrate the potential short-term positive impact of media coverage.
[90] SS_qII_qR	$c\beta_0 e^{-M(t)}SI$ with $M(t)=\max\left\{0,p_1I(t)+q_1I_q(t)+p_2\frac{dI(t)}{dt}+q_2\frac{dI_q(t)}{dt}\right\}$, where I_q represents isolated infected compartment.	The proposed model was then converted into a switching system, where the transmission probability is given by $\beta=e^{-\epsilon M_1(t)}\beta_0$ with $\epsilon=\begin{cases}0, & S-S_c(I,I_q)\le 0,\\ 1, & S-S_c(I,I_q)>0.\end{cases}$
[84] SIR	$\beta e^{-\alpha\epsilon I}SI$ with $\epsilon=\begin{cases}0, & I<I_c,\\ 1, & I>I_c.\end{cases}$	The system stabilizes at either the equilibrium of the two subsystems or the new endemic state induced by the on-off media effect, depending on the threshold levels.

Note: GAS stands for globally asymptotically stable, while LAS stands for locally asymptotically stable.

changes are activated only when $S > S_c$. They found that although the media and psychological impact do not affect the epidemic threshold, they delay the epidemic peak and result in a relative small outbreak size (or low equilibrium level of infected individuals). This kind of modeling can show that during disease outbreaks, the effect of behavioral changes is not always present. A Filippov epidemic model is also proposed to capture the impact of behavior changes driven by media coverage during the spread of an infectious disease. For example, Wang and Xiao [84] extend existing models by introducing a piecewise continuous transmission rate, where an exponentially decreasing function takes effect once the number of infected individuals surpasses a critical threshold, see details in Table 2.

In this line of research, some studies have incorporated traditional surveillance data for analysis. For example, Song and Xiao [69] parameterized the proposed model on the basis of the 2009 A/H1N1 pandemic influenza data in Shaanxi province, China, and estimated the basic reproduction number and the time delay. Xiao *et al.* [90] observed that behavior change driven by media impact switched off almost as the epidemic peaked by parameterizing the proposed model with the 2009 A/H1N1 influenza outbreak data in the Shaanxi province. Collinson and Heffernan [18] examined various functions $f_i(I,p_i)$ ($i=1,2,3$) to modify the incidence rate $\beta f_i(I,p_i)SI$ within the framework of the classic SEIR model, where

$$f_1(I,p_1)=e^{-p_1\gamma I},\quad f_2(I,p_1)=\frac{1}{1+p_2I^2},\quad f_3(I,p_3)=1-\frac{I}{p_3+I}.$$

They conducted a comparative analysis of these functions and investigated epidemic outcomes parameterized for an influenza outbreak. Their findings suggest that the choice of function representing the effects of media during an epidemic significantly influences the outcomes of a disease model, including the variability in key epidemic measurements. Mitchell and Ross [51] proposed a new, simple function $f_4(I,p_4)=1-p_4I$ to represent the reduction in disease transmission due to behavior changes driven by media reports. They incorporated this function into a deterministic SEIR model and combined it with a corpus of over 2.9 million geolocated, flu-related tweets. Their results show that this function provides a better fit to incidence data compared to models without behavior change, as well as to the previously proposed media functions $f_1(I,p_1)$ and $f_2(I,p_2)$.

3.3 Models considering the level of information

Media reports and social media play a significant role in shaping public opinions, attitudes, and perspectives. As the number of people accessing the internet increases, online media and social platforms are rapidly becoming major sources for news, health-related information, and advice. Correlations have been observed between flu-related tweets extracted using the Twitter API or disease-related media coverage and the actual number of reported cases [3,92]. In light of this, Yan *et al.* [92] assumed that disease transmission follows the SEIR model, treating media coverage as an independent compartment, $M(t)$,

and incorporating an incidence rate of the form $\beta e^{-pM(t)}S(t)I(t)$. It is assumed that the rate of change in M is associated with the number of new infections and decays over time at a rate μ. The resulting model is expressed as

$$\begin{cases} \dfrac{dS(t)}{dt} = -e^{-pM(t)}\beta\dfrac{S(t)I(t)}{N}, \\ \dfrac{dE(t)}{dt} = e^{-pM(t)}\beta\dfrac{S(t)I(t)}{N} - \sigma E(t), \\ \dfrac{dI(t)}{dt} = \delta E(t) - \gamma I(t), \\ \dfrac{dM(t)}{dt} = \eta(t)\delta E(t) - \mu M(t). \end{cases}$$

Here, $1/\delta$ represents the latent period, and the reporting rate $\eta(t)$ is a piecewise function defined as

$$\eta(t) = \begin{cases} \eta_0 \exp\big(q(T_2 - t)\big), & t \in T_{11} \subset T_1, \\ \eta_1 \exp\big(q(T_2 - t)\big), & t \in T_{12} \subset T_1, \end{cases}$$

where T_1 denotes the total time interval, T_2 is the period during which the number of daily news items increased significantly, and T_{11} (T_{12}) corresponds to weekends (weekdays). The parameter η_0 and η_1 represent the basic media reporting rates during weekends and weekdays, respectively, with $\eta_0 < \eta_1$. The study fitted the model to the daily number of newly hospitalized cases during the A/H1N1 influenza outbreak in Shaanxi Province in 2009 and the corresponding daily news articles from eight major websites. Based on this analysis, it was found that increasing T_2 or η_1, or decreasing δ, can effectively reduce the cumulative number of hospitalizations. Based on this modeling approach, various forms of media coverage $M(t)$ and different kind of functions to adjust the incidence rate have been proposed [39, 70, 95, 96], as detailed in Table 3. There is also some work that investigates the influence of media on the dynamics of vector-borne diseases [32, 49]. Additionally, to analyze the effect of twitter, Pawelek *et al.* [55] proposed a model that divides the population into susceptible (S), exposed (E), and infected (I) compartments. Individuals in each compartment are assumed to tweet about influenza at rates μ_1, μ_2, and μ_3, respectively. To account for the impact of public awareness through social media, the number of influenza-related tweets at time t is denoted by $T(t)$. An exponential function $e^{-\alpha T}$ was incorporated into the model to adjust the incidence rate, reflecting the behavioral changes after reading tweets about influenza. The corresponding equations are formulated as follows:

$$\begin{cases} \dfrac{dE(t)}{dt} = e^{-\alpha T}\beta SI - \rho E, \\ \dfrac{dI(t)}{dt} = \rho E - \gamma I, \\ \dfrac{dT(t)}{dt} = \mu_1 S + \mu_2 E + \mu_3 I - \tau T. \end{cases}$$

Table 3: Incorporating an independent media coverage compartment into classical epidemic models.

Reference, basic model	Media function M	Incidence function	Main conclusion
[96] SEIRM	$\frac{dM}{dt}=\rho\sigma E-\delta M$, where ρ represents the reporting rate of the newly observed individuals (σE).	$e^{-\alpha_1 I-\alpha_2 M}\beta SI$ or $\frac{\beta SI}{1+\alpha_1 I+\alpha_2 M}$.	The disease-free equilibrium is GAS if $R_0<1$ and unstable otherwise. A unique, LAS endemic equilibrium exists if $R_0>1$.
[70] SEISM	$\frac{dM}{dt}=\delta I(t)-\mu M$.	$\beta e^{-\alpha M}SI$.	The media described feedback cycle, from infection to the level of mass media and back to disease incidence can result in periodic oscillations.
[95] SS_qEE_qIHRM	$\frac{dM}{dt}=\eta(\delta_I I+\delta_q E_q)-\mu_M M$, where E_q represents quarantined exposed individuals and $\delta_I I+\delta_q E_q$ denotes the number of newly hospitalized cases.	$e^{-pM}\beta S(I+\theta E)$ (Quarantine rate $\lambda_M SM$ and $\lambda_M EM$ are also incorporated to capture the transition of S and E to S_q and E_q, respectively, as a result of media reports).	Sensitivity analysis indicates that improving media responsiveness and public awareness can significantly advance the peak time and reduce the peak size of infections in the early COVID-19 outbreak.
[39] SEISM	$\frac{dM}{dt}=\frac{\delta\sigma E}{1+h\sigma E}-\mu_d M$, where σE represents the number of newly observed infectious individuals and h is a measure of the saturation effect of media reports.	$e^{-\alpha M}\beta SI$.	The saturation of media coverage may hardly influence on the dynamics in terms of inducing multiple endemic equilibria or bifurcations, but does affect the endemic infection level.

Note: GAS stands for globally asymptotically stable, while LAS stands for locally asymptotically stable.

Without considering natural birth and death rates, assuming a constant susceptible population, the system exhibits a Hopf bifurcation when a key parameter reaches and crosses a threshold curve, indicating the potential for multiple influenza outbreaks. Numerical simulations, sensitivity analyses on tweet-related parameters, and comparisons with surveillance data from the 2009 H1N1 flu outbreak in England and Wales reveal that social media platforms like Twitter can effectively indicate seasonal influenza trends and impact disease dynamics.

Such models typically assume that the impact of behavioral changes is related to the number of infections, the rate of change in infections, or media coverage, all of which

are directly reflected in the incidence rate. While this makes the model simpler, it fails to capture the trend of behavioral changes over time. Furthermore, these models do not describe the evolution of behavior and neglect the influence of the costs associated with adopting behavioral changes.

3.4 Models with behavioral change described by neural networks

The above modeling approaches often rely on specific assumptions that need to be carefully validated. Simple assumptions enhance tractability but fit poorly, while complex ones improve fitting but reduce efficiency and generalization. Behavioral change models must strike a delicate balance by leveraging available data and theoretical insights on complex social and behavioral phenomena while maintaining key modeling properties, such as computational tractability and simplicity.

Recent advances in machine learning models, based on data generated during the pandemic, offer promising tools to enhance the analysis of disease models [60]. Specially, deep neural networks can be embedded in differential equations [16] to learn unknown mechanisms and offer new perspectives on solving traditionally challenging problems. Furthermore, data-driven methods, such as symbolic regression, sparse identification of nonlinear dynamical systems (SINDy) [11], and dynamic mode decomposition [11], have been developed to identify the simplest analytic expressions that describe scientific, engineering, and real-world data. Building on this, Song *et al.* [71] proposed a two-step recovering-explaining framework that combines deep learning methods with data-driven approaches to uncover the exact expressions of unknown behavioral change mechanisms in transmission dynamics models. The corresponding neural differential equation model is

$$\begin{cases} \dfrac{dS}{dt} = -\text{abs}\big(NN(I,R)\big)\dfrac{S}{N}, \\ \dfrac{dI}{dt} = \text{abs}\big(NN(I,R)\big)\dfrac{S}{N} - \gamma I, \\ \dfrac{dR}{dt} = \gamma I, \\ \dfrac{dH}{dt} = \text{abs}\big(NN(I,R)\big)\dfrac{S}{N}, \end{cases}$$

where $NN(I,R)$ represents the neural network used to learn the behavior change impact function, and H denotes the accumulated cases. Their framework was applied to COVID-19 data from Ontario to uncover the behavioral change mechanisms. It achieves a balance between the learning capacity of neural networks and the interpretability of transmission dynamics models, offering a powerful approach for exploring hidden mechanisms with limited epidemic data and addressing other relevant issues in epidemiological modeling.

Kuwahara and Bauch [35] developed a universal delay differential equation based on the standard SIR model for COVID-19

$$\begin{cases} \dfrac{dS(t)}{dt} = -\beta\big(M(t-\tau_1)\big)S(t)I(t), \\ \dfrac{dI(t)}{dt} = \beta\big(M(t-\tau_1)\big)S(t)I(t) - \gamma I, \\ \dfrac{dM(t)}{dt} = e^{-\delta t} f\big(I(t-\tau_1), \Delta I(t-\tau_2), M(t), R(t)\big), \end{cases}$$

where the impact of mobility (i.e. contact rate) on the transmission rate is modeled using neural networks to represent $\beta(M)$ and $f(I,\Delta I,M,R)$. Here, M represents the relative difference in mobility compared to the baseline, while $\Delta I(t)$ denotes the change in I between the current time t and a previous time $t-\tau_2$. They tested the ability of the universal differential equation (UDE) to predict second pandemic waves and found that UDEs can effectively learn the coupled dynamics of behavior change and disease spreading, enabling predictions of second waves across various populations. This is possible when the model is provided with learning biases that incorporate simple assumptions about disease transmission and population responses. During the pandemic, individuals may decide whether to travel to other regions, and such behavioral changes can influence disease transmission. Rajas-Campus *et al.* [63] incorporated a novel term into the SIR model, utilizing a deep neural network to learn the influence of neighboring regions on a target region. This approach improves prediction accuracy without relying on complex assumptions about the effects of adjacent regions. Additionally, the SINDy algorithm is employed as a post hoc tool to derive an algebraic representation of the function learned by the deep neural network (DNN).

With the help of deep learning, we can achieve excellent data fitting and prediction; however, the underlying functional form of the data, such as the true incidence function, cannot be effectively revealed. Combining transmission dynamics models with deep learning – integrating both interpretative and predictive approaches – is a promising yet underexplored area in mathematical epidemiology, with many challenges remaining.

4 Modeling distinct behaviors and transitions in subpopulations

To elucidate the specific trends of behavioral evolution, the population can be stratified based on differences in individuals' behavioral patterns, such as dividing into two subgroups: those adopting non-pharmaceutical interventions (NPIs) and those not adopting NPIs. The subgroup adopting NPIs is characterized by a lower infection rate or susceptibility. In exploring disease transmission, it is essential to simultaneously consider transitions between different behavioral subgroups to develop a co-evolutionary model that integrates behavioral changes and disease transmission dynamics.

4.1 Behavioral transitions driven by the total number of subgroups

When considering behavioral subgroups, the most intuitive approach is to assume that the rate of behavioral change acquisition is related to the total number of individuals adopting the behavioral change. For example, Funk *et al.* [23] proposed an SIRS model that simultaneously incorporates behavioral changes and disease transmission

$$\begin{cases} \dfrac{dS_-}{dt} = -(I_- + \sigma_I I_+)\beta\dfrac{S_-}{N} + \delta R_- - \alpha(S_+ + I_+ + R_+)\dfrac{S_-}{N} + \lambda S_+, \\ \dfrac{dI_-}{dt} = (I_- + \sigma_I I_+)\beta\dfrac{S_-}{N} - \gamma I_- - \omega I_- - \alpha(S_+ + I_+ + R_+)\dfrac{I_-}{N} + \lambda I_+, \\ \dfrac{dR_-}{dt} = \gamma I_- - \delta R_- - \alpha(S_+ + I_+ + R_+)\dfrac{R_-}{N} + \lambda R_+, \\ \dfrac{dS_+}{dt} = -(I_- + \sigma_I I_+)\sigma_S\beta\dfrac{S_+}{N} + \phi\delta R_+ + \alpha(S_+ + I_+ + R_+)\dfrac{S_-}{N} - \lambda S_+, \\ \dfrac{dI_+}{dt} = (I_- + \sigma_I I_+)\sigma_S\beta\dfrac{S_+}{N} - \varepsilon\gamma I_+ + \omega I_- + \alpha(S_+ + I_+ + R_+)\dfrac{I_-}{N} - \lambda I_+, \\ \dfrac{dR_+}{dt} = \varepsilon\gamma I_- - \phi\delta R_+ + \alpha(S_+ + I_+ + R_+)\dfrac{R_-}{N} - \lambda R_+. \end{cases} \tag{4.1}$$

In this model, the subscripts "$-$" and "$+$" denote individuals without and with disease awareness, respectively, where the disease-aware population adopts NPIs. The unaware population transitions to the aware portion of the population at a rate of α due to the spread of awareness, while awareness is lost or forgotten at a rate of λ. And unaware infected individuals can independently become aware at a transition rate ω, without requiring contact with others. Besides, parameters σ_I and σ_S adjust the transmission rate of infected individuals and the infection probability of susceptibles due to behavioral changes; ε and ϕ adjust the recovery rate of infected individuals and the immunity loss rate of recovered individuals. Theoretically, thresholds for disease transmission and information dissemination are defined. Given the complexity of the high dimension system, numerical analyses reveal that the threshold for information dissemination affects the number of infected individuals at the endemic equilibrium. Building on this framework, Agaba *et al.* [1] extended the model by considering spontaneous awareness acquisition not only among infected individuals (represented by parameter ω in the aforementioned model (4.1), now denoted as ω_2) but also among susceptibles and recovered individuals, with respective rates ω_1 and ω_3. They conceptualized this spontaneous awareness as "public" awareness. Additionally, the model assumed that the rates of awareness acquisition and loss differ among susceptibles, infected, and recovered individuals, denoted by $\alpha_1, \alpha_2, \alpha_3$ for acquisition rates, and $\lambda_1, \lambda_2, \lambda_3$ for loss rates, respectively. This process was defined as the influence of "private" awareness, wherein individuals transition from being unaware to aware of the disease at rate α_j and subsequently lose awareness at rate λ_j. Numerical analyses demonstrated that the parameters ω_i and α_i (i=1,2,3) significantly affect the stability of the disease-free equilibrium, highlighting that both "private" and "public" awareness influence the disease threshold. Note that, a limitation of such

models is the assumption that awareness acquisition is related to the number of recovered individuals with disease awareness, and not to the recovered individuals without disease awareness. To address this, Kiss *et al.* [33] assume that awareness acquisition by public information is related to the total number of recovered/treatment individuals, regardless of whether they have disease awareness. They divided the population into susceptible non-responsive S_{nr}, susceptible responsive S_r, infectious non-responsive I_{nr}, infectious responsive I_r and treatment class T. They assumed that the transition rate from S_{nr} to S_r (from I_{nr} to I_r), driven by information dissemination through direct contact between individuals, is given by

$$\alpha_s S_{nr}\frac{S_r+I_r+T}{N} \quad \left(\alpha_i I_{nr}\frac{S_r+I_r+T}{N}\right),$$

while the transition driven by population-wide transmission of information is given by

$$\delta_s S_{nr}\frac{I_{nr}+I_r}{K+I_{nr}+I_r} \quad \left(\delta_i I_{nr}\frac{I_{nr}+I_r}{K+I_{nr}+I_r}\right).$$

They provided a comprehensive characterization of the global dynamics of the model, and demonstrated that the parameter space can be partitioned into three regions, each corresponding to a distinct global attractor of the system: one of the two disease-free equilibria or the endemic equilibrium.

Additionally, Li and Dong [36] assumed that the disease follows the SIR model and only divided the susceptible population into two classes: disease-unaware individuals (S_1) and disease-aware individuals (S_2). Mass communication induces transitions from S_1 to S_2 at a rate γ. The effect of interpersonal communication is modeled by assuming that individuals in S_1 can acquire disease-related information through interactions with either S_2 or$I$, at rate $\delta S_1 S_2$ and $(1-p)\beta_1 S_1 I$, respectively. Here, β_1 represents the effective contact rate from infected to disease-unaware susceptible, and $(1-p)\beta_1$ denotes the probability of disease awareness transmission per contact by an infective. The corresponding model is as follows:

$$\begin{cases} \dfrac{dS_1}{dt} = A_1 - dS_1 - \gamma S_1 - \delta S_1 S_2 - \beta_1 S_1 I, \\ \dfrac{dS_2}{dt} = A_2 - dS_2 + \gamma S_1 + \delta S_1 S_2 + (1-p)\beta_1 S_1 I - \beta_2 S_2 I, \\ \dfrac{dI}{dt} = p\beta_1 S_1 I + \beta_2 S_2 I - dI - \alpha I - vI, \\ \dfrac{dR}{dt} = vI - dR, \end{cases}$$

where $p\beta_1 > \beta_2$ since S_2 may be infected at a lower rate than those S_1. The transmission rate of information is faster than the infected rate of susceptible individuals, i.e. $\delta > p\beta_1 > \beta_2$. It has been proven that the disease-free equilibrium is stable if $R_0 < 1$ and unstable if $R_0 > 1$. Note that, this model neglects the loss of disease awareness.

4.2 Behavioral transitions driven by information diffusion

Except for categorizing behavioral subgroups, some studies have introduced media coverage as an independent compartment M and assumed that it influences the rate of behavioral change [73]. For instance, in the context of the SIS model, the susceptible population is divided into those without disease awareness (S_-) and those with disease awareness (S_+), where S_+ individuals adopt NPIs, reducing their infection probability compared to S_-. The conversion rate from S_- to S_+ is assumed to be linearly dependent on M, and S_+ converts to S_- at a constant rate λ_0 [67], and the model is formulated as

$$\begin{cases} \dfrac{dS_-}{dt} = A-\beta S_- I - dS_- + (1-p)\gamma I - \lambda S_- M + \lambda_0 S_+, \\ \dfrac{dS_+}{dt} = -\beta_1\beta S_+ I - dS_+ + p\gamma I + \lambda S_- M - \lambda_0 S_+, \\ \dfrac{dI}{dt} = \beta S_- I + \beta_1\beta S_+ I - \gamma I - \alpha I - dI, \\ \dfrac{dM}{dt} = k\alpha I - \mu_0 M, \end{cases} \tag{4.2}$$

where $0<\beta_1<1$. The basic reproduction number R_0 was theoretically calculated and found to be independent of β_1. It was proven that when $R_0<1$, the disease-free equilibrium is locally asymptotically stable, while for $R_0>1$, the system admits a unique endemic equilibrium. Furthermore, as the parameter k varies, the system undergoes a Hopf bifurcation, leading to periodic solutions. The results indicate that behavioral changes do not affect R_0 but can lead to periodic solutions in the system. The special case where $\beta_1=0$ and $p=0$ was also investigated by Misra *et al.* [50]. Building on this modeling approach, Greenhalgh *et al.* [26] assumed that the conversion rate from S_- to S_+ is given by $\lambda S_- M/(k+M)$, and the transmission rate between S_+ and I is $\beta S_+ I/(1+\beta_1 M)$. This model retains the same basic reproduction number R_0 as the previous model (4.2) and theoretically proves that endemic equilibrium exists only when $R_0>1$. Zou *et al.* [97] assumed that the conversion rate from S_- to S_+ is given by $\lambda S_- M/(1+kM)$ and individuals in S_+ are not susceptible to infection. They also considered the impact of the media coverage density level μ_0 on the disease dynamics influenced by other regions. In their model, $M(t)$ evolves according to the equation

$$\frac{dM}{dt} = \mu_0 + \mu I - \mu_0 M.$$

It is found that the disease free equilibrium is also locally asymptotically stable when $R_0<1$. Li and Xiao [38] assumed that the disease follows the SIR transmission model. Disease-unaware individuals S_1, I_1, and R_1 interact with media at rates λSM, λIM, and λRM, respectively, transitioning into disease-aware individuals S_2, I_2, and R_2. Considering time variation between information dissemination, epidemiological and demographic processes, they obtained a slow-fast system by reasonably introducing a sufficiently

small quantity and obtained the similarity between the basic dynamical behaviors of the slow system and that of the full system. Rai *et al.* [61] divided the susceptible population into individuals without disease awareness S and those with disease awareness A, while also considering symptomatic I_s and asymptomatic I_a infected individuals. They assumed that the cumulative number of social media advertisements, $M(t)$, evolves according to the equation

$$\frac{dM}{dt} = r\left(1-\theta\frac{A}{w+A}\right)I_s - r_0(M-M_0),$$

where M_0 stands for the baseline number of social media advertisements. Additionally, the incidence rates between S and I_s, and between S and I_a, are given by

$$\beta_1\left(1-c_{ms}\frac{M}{p+M}\right)SI_s, \quad \text{and} \quad \beta_2\left(1-c_{ma}\frac{M}{p+M}\right)SI_a.$$

They calibrated the proposed model using the cumulative confirmed COVID-19 cases for India and found that the basic reproduction number for India is greater than one. Furthermore, they concluded that to reduce the disease burden in India, non-pharmaceutical intervention strategies should be effectively implemented to decrease the basic reproduction number below one, based on sensitivity analysis. Furthermore, Tiwari *et al.* [81] considered highly active aware individuals A_h, such as healthcare workers and educated individuals, and less active aware individuals A_l, such as uneducated or careless individuals. Unaware susceptible individuals S become aware through global awareness at rates $(1-b)\lambda SM/(p+M)$ for the highly active class (A_h) and $b\lambda SM/(p+M)$ for the less active class (A_l), or through local awareness at rates $(1-c)\rho SA_h$ and $c\rho SA_h$, respectively. Individuals in A_h and A_l may lose awareness and become susceptible again at rates λ_{01} and λ_{02}. They also calibrated the model using the cumulative confirmed COVID-19 cases for India and found that both global and local awareness strategies can be effectively implemented to manage the burden of the COVID-19 pandemic. Similarly, Collinson *et al.* [19] refined the susceptible population by subdividing it into fully susceptible individuals (S), susceptible individuals practicing social distancing (S_1), and isolated susceptible individuals (S_2), where S_2 individuals cannot be infected. A vaccination compartment V was further introduced, assuming that the transitions among these susceptible subgroups, as well as their vaccination rates, are linearly dependent on media coverage. And the rate of change in media coverage (M) is directly proportional to the number of new cases. The basic reproduction number R_0 was derived and shown to be independent of parameters related to behavioral changes. It was proven that the disease is eradicated when $R_0 < 1$. Numerical analysis further showed that vaccination uptake and social distancing practices reduce the impact of an epidemic, while waning behavior diminishes these benefits. Chang *et al.* [15] divided the susceptible population into those without active isolation and protection awareness S and those with such awareness S_m. They also included asymptomatic or symptomatic unconfirmed infections I,

who are infectious but not under isolation, and patients I_m who practice self-protection or self-isolation, though without formal isolation treatment. The model incorporates three types of effective information: positive emotions (M_1) from media coverage, negative emotions (M_2), and regulatory information (M_3) that mitigates public negative emotions. They defined the growth function of medical resources with Logistic mapping, $Y(t)$, as

$$Y(t)=\frac{M_1(t)-M_2(t)+M_3(t)}{K+M_1(t)+M_3(t)}r\frac{w(t)\big(W-w(t)\big)}{W},$$

where w represents local medical resources. The transition rate from S to S_m (I to I_m) is assumed to be $\varphi_1 SY$ ($\varphi_2 IY$). The model was validated using reported data from the COVID-19 pandemic in Wuhan, and the relationship between R_0 and the model parameters was analyzed. Numerical analysis showed that reducing the implementation rate of negative information generated by confirmed cases, increasing the implementation rate of policies and regulations information, or gradually increasing the inhibition of negative information by policies and regulations can significantly reduce the cumulative number of confirmed cases. More details about the modeling of media and its effects can be found in the review by Sooknanan and Seemungal [73], which corresponds to the design of media coverage discussed in the previous section and this section.

This modeling approach explicitly incorporates behavioral evolution; however, the increased dimensions of compartmental models, resulting from the detailed representation of behavioral patterns, make theoretical analysis challenging. Moreover, most models assume that disease awareness decays exponentially, whereas in reality, factors such as the current state of the epidemic and the cost of behavioral changes require further investigation.

5 Game-theoretic modeling of infectious disease dynamics and behavioral change

Behavioral decision-making does not follow simple linear logic but instead involves a complex trade-off process among multiple factors. Evolutionary game theory provides a precise framework for modeling this intricate decision-making process. Also known as evolutionary game theory, it applies the mathematical principles of game theory to biological contexts. This concept was first introduced in 1973 by Smith and Price [68], who formalized biological competition within ecosystems as strategies for analysis and quantified them into mathematical standards to predict the trajectory of competitive strategies. Within the dynamic framework of evolutionary biology, evolutionary game theory incorporates the strategies and analytical approaches of game theory, with a focus on the strategy changes that arise during the evolutionary dynamics of individuals and populations [53]. This theory has successfully explained and complemented Darwin's theory of evolution, particularly in terms of cooperative behavior. It has gradually found applications across various fields, including human sociology [75] and biology [62].

5.1 Nash equilibrium strategy

In game theory, the Nash equilibrium represents one of the most fundamental and widely used solution concepts for non-cooperative games. It describes a state in which no player can improve their payoff by unilaterally deviating from their current strategy, assuming that all other players' strategies remain fixed [2]. Bauch and Earn [8] applied the Nash equilibrium concept to vaccination strategies based on the basic SIR model. They defined two strategies: Vaccinator and Non-vaccinator. The payoffs for a vaccinated individual and an unvaccinated individual are $-r_v$ and $-r_i\pi_p$ respectively, where π_p denotes the probability that an unvaccinated individual will eventually become infected, given a vaccine coverage level p in the population. The expected payoff for adopting a mixed strategy, where an individual chooses to vaccinate with probability P, is expressed as

$$E(p,P)=P(-r_v)+(1-P)(-r_i\pi_p).$$

The corresponding epidemiological model is

$$\begin{cases} \dfrac{dS}{dt}=\mu(1-p)-\beta SI-\mu S, \\ \dfrac{dI}{dt}=\beta SI-\gamma I-\mu I, \\ \dfrac{dR}{dt}=\mu p+\gamma I-\mu R, \end{cases}$$

where p is the vaccine uptake level. The analysis focuses on the case where $R_0>1$. Under this case, π_p is defined as

$$\pi_p=\frac{R_0(1+f)\hat{S}\hat{I}}{R_0(1+f)\hat{S}\hat{I}+f\hat{S}}=1-\frac{1}{R_0(1-p)},$$

where $f=\mu/\gamma$ and $(\hat{S},\hat{I})$ is denotes the endemic equilibrium of the system. Using this framework, they identified the (convergently stable) Nash equilibrium for the vaccination strategy. This type of modeling defined the probability that an unvaccinated individual would eventually become infected solely based on the stable (equilibrium) state of the disease model, while ignoring the time-varying dynamics of the process.

5.2 Behavioral change described by replicator dynamics

In mathematics, the replicator equation is a deterministic and non-linear, game dynamic commonly used in evolutionary game theory [31]. Applied to disease transmission, the general form is

$$\frac{dx_i}{dt}=x_i[\pi_i(x)-\overline{\pi}(x)], \tag{5.1}$$

where x_i is the proportion of individuals adopting strategy i, π_i is the fitness (or payoff) of strategy i, and $\overline{\pi}(x)=\sum x_i\pi_i(x)$. It models the effects of natural selection by describing

how the frequencies of strategies evolve over time, which can describe behavior changes in the disease transmission process. For example, Saad-Roy and Traulsen [65] proposed a behavioral – epidemiological model to describe individual adherence to NPIs based on the replicator equation. They employed the SIRS framework to model disease progression, incorporating the impact of NPIs as a reduction in the transmission rate β. The adjusted transmission rate under NPIs is defined as $b\beta$, where $0 \leq b < 1$ quantifies the effectiveness of NPIs. They further defined $b = px_A + (1-x_A)$, where p is the relative probability of transmission, x_A is the fraction of adherers A, and $1-x_A$ is the fraction of nonadherers N. The dynamics of x_A are modeled by replicator equation, with the corresponding payoff matrix given by

$$P = \begin{array}{c} \\ N \\ A \end{array} \begin{array}{c} \begin{array}{cc} N & A \end{array} \\ \begin{pmatrix} -\beta I\xi & -p\beta I\xi \\ -p\beta I\xi - c & -p^2\beta I\xi - c \end{pmatrix} \end{array}, \tag{5.2}$$

where ξ represents the perceived infection risk and c is the cost of adhering NPIs. Thus, the average payoff for nonadheres and adheres are

$$\begin{aligned} \pi_N &= -\beta I\xi(1-x_A) - p\beta I\xi x_A, \\ \pi_A &= (-p\beta I\xi - c)(1-x_A) + (-p^2\beta I\xi - c)x_A, \end{aligned}$$

respectively. The resulting model is given as

$$\begin{cases} \dfrac{dS}{dt} = \mu - [px_A + (1-x_A)]\beta SI - \mu S + \delta(1-S-I), \\ \dfrac{dI}{dt} = [px_A + (1-x_A)]\beta SI - \gamma I - \mu I, \\ \dfrac{dx_A}{dt} = x_A\left[\pi_A - \left(x_A\pi_A + (1-x_A)\pi_N\right)\right] = x_A(1-x_A)(\pi_A - \pi_N), \end{cases}$$

where $R = 1-S-I$ and $x_A\pi_A + (1-x_A)\pi_N$ is the average payoff of whole susceptible population. They found, surprisingly, that in the equilibrium with partial NPI adherence, the number of infections is independent of the transmission rate. In other words, there exists an equilibrium (S_*, I_*, x_*) with $0 < x_* < 1$, where I_* is independent of the parameter β. Moreover, they identified parameter regions where individual incentives might diverge from the collective interests of society by examining the payoff difference between the stable equilibrium and that of a population with complete adherence. Martcheva *et al.* [48] proposed a simpler SIS model framework with a constant human population, assuming that individuals practicing strict social distancing will not be infected. The dynamics of the fraction of individuals practicing strict social-distancing (x_A) are also governed by the replicator equation. The corresponding payoff matrix is

$$P = \begin{array}{c} \\ N \\ A \end{array} \begin{array}{c} \begin{array}{cc} N & A \end{array} \\ \begin{pmatrix} \delta_0 - cI & -cI \\ -r_s & \delta_0 - r_s \end{pmatrix} \end{array}, \tag{5.3}$$

where δ_0 represents the strength of social norms to adhere to a strategy, r_s is the cost of maintaining strict social-distancing and I is the proportion of infected individuals. Thus, the average payoff of individuals practicing or not practicing strict social-distancing are

$$\begin{aligned}\pi_A &= (\delta_0 - r_s)x_A - r_s(1-x_A),\\ \pi_N &= -cIx_A + (\delta_0 - cI)(1-x_A).\end{aligned}$$

Compared to the payoff matrix (5.2), the matrix (5.3) includes the strength of social norms, and assumes that if a non-adherer is the focal player, the payoff induced by the perceived risk of infection is the same when interacting with either another non-adherer or an adherer. The resulting model is

$$\begin{cases}\dfrac{dI}{dt} = (1-x_A)\beta I(1-I) - (\mu+\gamma)I,\\ \dfrac{dx_A}{dt} = x_A\big[\pi_A - \big(x_A\pi_A + (1-x_A)\pi_N\big)\big] = x_A(1-x_A)(\pi_A - \pi_N),\end{cases}$$

where $S = 1-I$. They analyzed the existence and stability of all possible equilibria and demonstrated that a Hopf bifurcation can occur. Their findings suggest that while the disease could be eradicated if everyone adopts strict social-distancing measures, the more realistic outcome is a persistent level of infection coexisting with a moderate degree of social-distancing adherence. Glaubitz and Fu [25] proposed a model that integrates the classical SIR framework with a replicator equation to capture the evolution of social distancing behavior. They defined the payoff of adopting social distancing as $\pi_{sd} = -C_{sd}$, where C_{sd} is the perceived cost of social distancing at each time t. For individuals not practicing social distancing, the payoff is given by

$$\pi_{nsd} = -C_I\big[1-\exp\big(-\beta I(t)\big)\big],$$

where C_I denote the perceived cost of infection, and the risk of infection during the time interval $(t,t+1)$ without social distancing is approximated as

$$1-\exp\left(-\beta\int_t^{t+1} I(\tau)d\tau\right) \approx 1-\exp\big(-\beta I(t)\big).$$

Here, they directly assumed that the payoff of one strategy is the same regardless of the strategy of the person they interact with. The corresponding payoff matrix is

$$P = \begin{array}{c} \\ N \\ A \end{array}\begin{array}{c} \begin{array}{cc} N & \quad A \end{array} \\ \begin{pmatrix} -C_I\big[1-\exp\big(-\beta I(t)\big)\big] & -C_I\big[1-\exp\big(-\beta I(t)\big)\big] \\ -C_{sd} & -C_{sd} \end{pmatrix} \end{array}.$$

Since each row of the matrix is identical, for simplicity, we will not list the payoff matrix further and instead directly present the payoffs for each strategy. The resulting model is

described by the following system of equations:

$$\begin{cases} \dfrac{dS}{dt} = -\beta(1-\mathcal{E})SI, \\ \dfrac{dI}{dt} = \beta(1-\mathcal{E})SI - \gamma I, \\ \dfrac{dR}{dt} = \gamma I, \\ \dfrac{d\mathcal{E}}{dt} = \omega\mathcal{E}(1-\mathcal{E})\tanh\left(\dfrac{\kappa}{2}\left(-C_{sd}+C_I(1-e^{-\beta I})\right)\right), \end{cases} \tag{5.4}$$

where ω represents a responsiveness parameter, which determins the time scale for updating the social distancing behaviour. k is a rationality parameter. They found that voluntary social distancing can significantly reduce the total number of infections, $R(\infty)$. Furthermore, when the cost of social distancing, C_{sd}, is reduced, it is possible to observe an initial decrease in $R(\infty)$, followed by an increase. Unlike the classic SIR model, which typically produces a single large wave of infections, the proposed model (5.4) can exhibit multiple waves with smaller peaks. Additionally, with the adoption of social distancing, I_{HI} (the number of infections at the point when herd immunity is reached) decreases significantly, as social distancing greatly reduces the overall number of infections.

5.3 Behavioral change described by imitation dynamics

In the context of games played in human societies, the spread of successful strategies is more likely to occur through imitation rather than inheritance [30]. Imitation dynamics is a common concept in game theory, centered on the idea of imitation, where individuals tend to adopt "successful" strategies (i.e. those with higher payoffs). The corresponding general imitation dynamics is given by the input–output model

$$\frac{dx_i}{dt} = x_i \sum_j [f_{ij}(x) - f_{ji}(x)]x_j, \tag{5.5}$$

where x_i is the proportion of individuals adopting strategy i, the product $x_i x_j$ represents the probability of randomly and independently sampling the revising player (who uses strategy S_j) and the potentially imitated player (who uses strategy S_i). The term $f_{ij} = f_{ij}(f_i, f_j)$ denotes the rate at which the S_j strategist switches to S_i, where f_i is the payoff of strategy i. In some cases, the equation describing imitation dynamics can be transformed into a replicator equation [30]. For example, if we set $f_{ij} = f_i$, the equation takes the form of a replicator equation. A classic example is Bauch's [7] seminal work in 2005, which explored the interactions between vaccine coverage, disease prevalence, and individual vaccination behavior. Due to the existence of herd immunity, the likelihood of an individual becoming infected largely depends on the number of vaccinated individuals in their surrounding population. In this context, individuals face a strategic choice

when deciding whether to vaccinate. To address this, Bauch developed an infectious disease model that integrates dynamic decision-making processes

$$\begin{cases} \dfrac{dS}{dt} = \mu(1-x) - \beta SI - \mu S, \\ \dfrac{dI}{dt} = \beta SI - \gamma I - \mu I, \\ \dfrac{dR}{dt} = \mu x + \gamma I - \mu R, \\ \dfrac{dx}{dt} = kx(1-x)[-r_v + r_i m I], \end{cases} \tag{5.6}$$

where x represents the proportion of the population vaccinated at birth, and its dynamic process is characterized by imitation dynamics. The expected payoffs for vaccinated and unvaccinated individuals are given by

$$f_v = -r_v, \quad f_n = -r_i m I,$$

respectively, where r_v and r_i represent the costs of vaccination and infection, and $mI(t)$ denotes the probability of infection faced by unvaccinated individuals. Here, we assume that the transition rate f_{nv} (f_{vn}) from vaccination to non-vaccination (or vice versa) is directly proportional to the payoff of not vaccinating (f_n) or vaccinating (f_v), respectively, i.e. $f_{nv} = kf_n$ and $f_{vn} = kf_v$. As a result, incorporating this assumption into Eq. (5.5) yields the last term in Eq. (5.6). Note that, the parameter m quantifies the sensitivity to changes in disease prevalence. Theoretical analysis reveals that when the rate of behavioral change k is high or the sensitivity parameter m is large, the system exhibits oscillations. Moreover, this model successfully reproduces the temporal patterns of vaccine coverage and disease prevalence observed during the pertussis vaccine scare in England and Wales in the 1970s. These findings demonstrate that using imitation dynamics to predict the dynamic changes in vaccination behavior within a population is both feasible and effective. Building on this foundation, various types of payoff functions have been developed, including nonlinear forms, those considering time delays, and integral forms (where payoffs depend on the cumulative impact of past vaccine side effects). For more details, see the review in [86]. For seasonal epidemics, individuals decide whether to vaccinate in the upcoming season by evaluating the overall situation from the previous season [4, 93]. Their decision-making process continues to follow the principles of imitation dynamics.

The integration of imitation dynamics into the analysis of NPIs has also seen significant development. For example, Pedro *et al.* [56] studied behavioral changes in the context of the COVID-19 pandemic within the framework of the basic SEIR model. They assumed that the proportion of individuals supporting public venue closures, $x(t)$, influences the incidence rate of the disease as $(1-C(t))\beta SI$, where

$$C(t) = \begin{cases} C_0, & x(t) \geq 50\%, \\ 0, & x(t) < 50\%. \end{cases}$$

The dynamics of $x(t)$ follow imitation dynamics, with payoffs determined by infection risk and the current overall economic loss L

$$\frac{dx}{dt}=x(1-x)(f_{sn}-f_{ns})=x(1-x)[-k\epsilon L-(-kwI)],\quad \frac{dL}{dt}=\alpha C(t)-\delta L,$$

where f_{sn} (f_{ns}) represents the transition rate from not supporting to supporting public venue closures (or vice versa). Using early 2020 COVID-19 data from the United States, the model was fitted to explore how the parameters k,ϵ,α, and δ influence the number of epidemic waves and the ratio of the second wave peak to the first. The analysis revealed that the second wave of COVID-19 could be interpreted as the result of nonlinear interactions between disease dynamics and societal behavior. Such models directly assume that the proportion x of individuals not adopting NPIs follows an imitation process, and this is then coupled directly with the incidence rate, overlooking the impact of the differential infection rates between susceptible individuals adopting and not adopting NPIs on the proportion x.

To explicitly characterize behavioral evolution, it is also possible to consider behavioral subgroups and use imitation dynamics to describe the transitions between these subgroups. As a basic example, we extend the classical SIR model (without birth and death rates) by dividing the susceptible population (S) into two subgroups: those adopting altered behavior (S_a) and those adopting normal behavior (S_n). We assume that the transition between S_n and S_a follows an imitation process. The resulting model is given as

$$\begin{cases}\dfrac{dS_n}{dt}=-\beta S_nI+S_nS_a(f_{na}-f_{an}), & \text{(5.7a)}\\ \dfrac{dS_a}{dt}=-\eta\beta S_aI+S_aS_n(f_{an}-f_{na}), & \text{(5.7b)}\\ \dfrac{dI}{dt}=\beta S_nI+\eta\beta S_aI-\gamma I, & \text{(5.7c)}\end{cases}$$

where β (or $\eta\beta$, with $0\le\eta<1$) is the transmission rate between S_n (S_a) and I,γ is the recovery rate, and the last term in the Eqs. (5.7a) and (5.7b) corresponds to the standard form of the imitation process in Eq. (5.5). The terms f_{na} (f_{an}) represent the transition rate from altered behavior to normal behavior (or vice versa), which is directly proportional to the payoff of adopting normal behavior (P_n) (adopting altered behavior (P_a)), i.e. $f_{na}=\omega P_n$ ($f_{an}=\omega P_a$), where ω can represent the rate of behavior change. The payoffs P_a and P_n are defined as

$$P_n=-c\beta I,\quad P_a=-c\eta\beta I-k,$$

where k is the constant cost associated with adopting altered behavior, and c represents the cost related to the perceived risk of infection. Note that, compartments S_n,S_a and I represent fractions of the population instead of absolute numbers. Let $S=S_n+S_a$ and define $x=S_n/S$ as the fraction of susceptible individuals adopting normal behavior. The model (5.7) can then be rewritten as

$$\begin{cases} \dfrac{dS}{dt} = -[x+\eta(1-x)]\beta SI, & \text{(5.8a)} \\ \dfrac{dI}{dt} = [x+\eta(1-x)]\beta SI - \gamma I, & \text{(5.8b)} \\ \dfrac{dx}{dt} = -x(1-x)(1-\eta)\beta I + \omega x(1-x)S[k-(1-\eta)c\beta I]. & \text{(5.8c)} \end{cases}$$

Let

$$\Omega = \{(S,I,x) \in R^3 \mid 0 \le S+I \le 1, S \ge 0, I \ge 0, 0 \le x \le 1\},$$

which is a positively invariant set of system (5.8). We can theoretically show that the final size and peak size of the system described by Eq. (5.8) are smaller than those of the classical SIR model (i.e. Eq. (5.8) with $x(t)=1$), as demonstrated in the following theorem. The proof of this theorem is provided in the appendix.

Theorem 5.1. *Assume the initial values satisfy $S_0 = S(0), I_0 = I(0) > 0$ and $0 < x(0) < 1$. For the system* (5.8)*, it holds that*

$$\lim_{t\to\infty} I(t) = 0, \quad \lim_{t\to\infty} x(t) = 1.$$

Compared to the classical SIR model, both the final size $(R(\infty)$ or $1-S(\infty))$ and the peak size of the first wave (I_{peak}) of the system (5.8) *are reduced, that is to say,*

$$\lim_{t\to\infty} S(t) = S_\infty \ge S_\infty^{\text{SIR}} = -\frac{\gamma}{\beta} LambertW\left[-\frac{\beta}{\gamma}\exp\left(-\frac{\beta}{\gamma}\left(S_0+I_0-\frac{\gamma}{\beta}\ln S_0\right)\right)\right],$$

and

$$I_{\text{peak}} < I_{\text{peak}}^{\text{SIR}} = I_0 + S_0 + \frac{\gamma}{\beta}\ln\left(\frac{\gamma}{\beta}\frac{1}{S_0}\right) - \frac{\gamma}{\beta},$$

where $1-S_\infty^{\text{SIR}}$ and $I_{\text{peak}}^{\text{SIR}}$ denote the final size and peak size of the classical SIR model, respectively.

To further analyze the impact of behavior change, we compare the final size $(R(\infty))$, the peak time and peak size of the first wave, and the number of waves in model (5.8) under different parameters related to behavior change (c, k, ω, and η) with those in the classic SIR model, as shown in Figs. 1-4. It is demonstrated that behavior change can reduce both the peak size of the first wave and the final size $(R(\infty))$. Specifically, Figs. 1-2(e-f) illustrate that a higher cost associated with the perceived risk of infection (higher c) and a faster rate of behavior change (higher ω) both lead to a smaller peak size and an earlier peak time of the first wave, and a greater number of waves. It follows from Figs. 3(e-f) that a higher effectiveness of adopting altered behavior (lower η) leads to a smaller peak size and an earlier peak time of the first wave, and a greater number of waves. Fig. 4(e) shows that a lower cost of adopting altered behavior (smaller k) results in a smaller peak size and an earlier peak time of the first wave. As k increases, the number of waves initially increases and then decreases, as illustrated in Fig. 4(f). Additionally, when k is very large, both the final size and the peak size of the first wave closely approach those

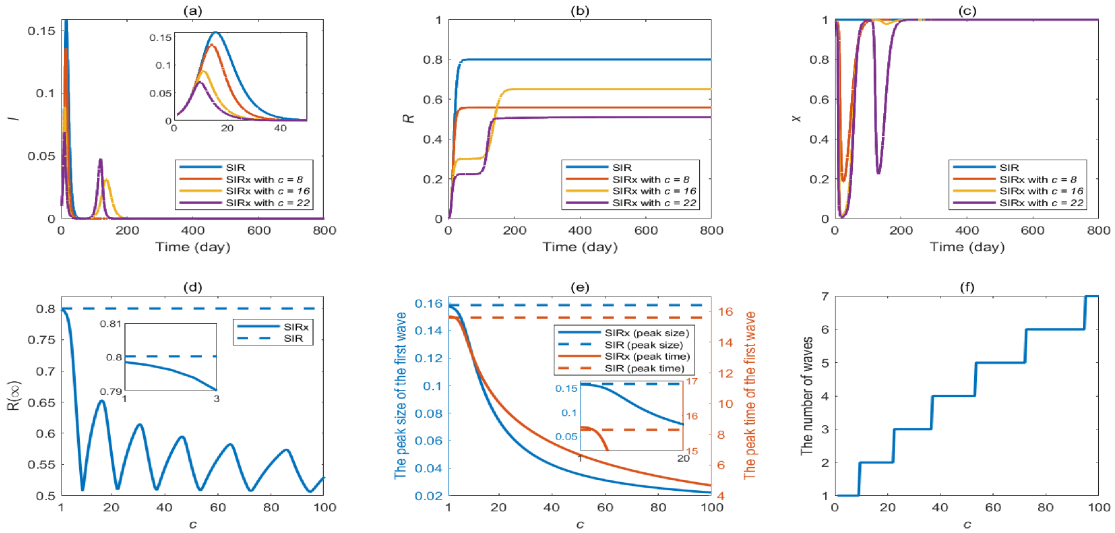

Figure 1: Numerical simulations regarding parameter c: (a)-(c) Time series of the classical SIR model and model (5.8) (denoted as "SIRx" in the figure) under different values of c. (b) Final size of the epidemic ($R(\infty)$) for model (5.8) as a function of parameter c. The dashed line represents the result under the classic SIR model. (e) Variation in the peak size and peak time of the first wave with parameter c. The dashed line represents the result under the classic SIR model. (d) Number of waves under different values of parameter c. The other parameters are fixed as follows: $\beta=0.6,\gamma=0.3,\eta=0.2,\omega=2,k=0.1$.

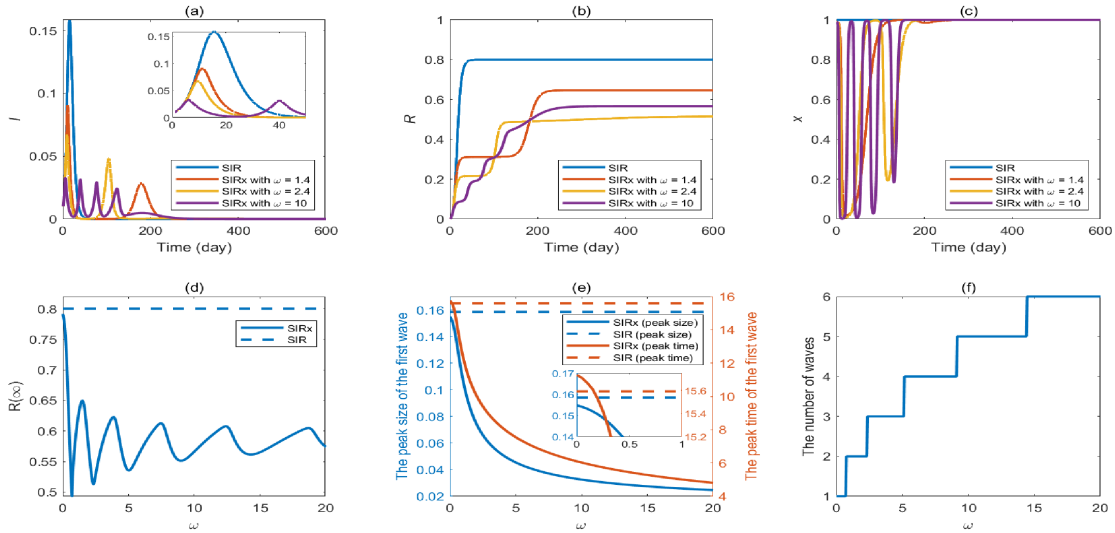

Figure 2: Numerical simulations regarding parameter ω: (a)-(c) Time series of the classical SIR model and model (5.8) (denoted as "SIRx" in the figure) under different values of ω. (b) Final size of the epidemic ($R(\infty)$) for model (5.8) as a function of parameter ω. The dashed line represents the result under the classic SIR model. (e) Variation in the peak size and peak time of the first wave with parameter ω. The dashed line represents the result under the classic SIR model. (d) Number of waves under different values of parameter ω. The other parameters are fixed as follows: $\beta=0.6,\gamma=0.3,\eta=0.2,c=20,k=0.1$.

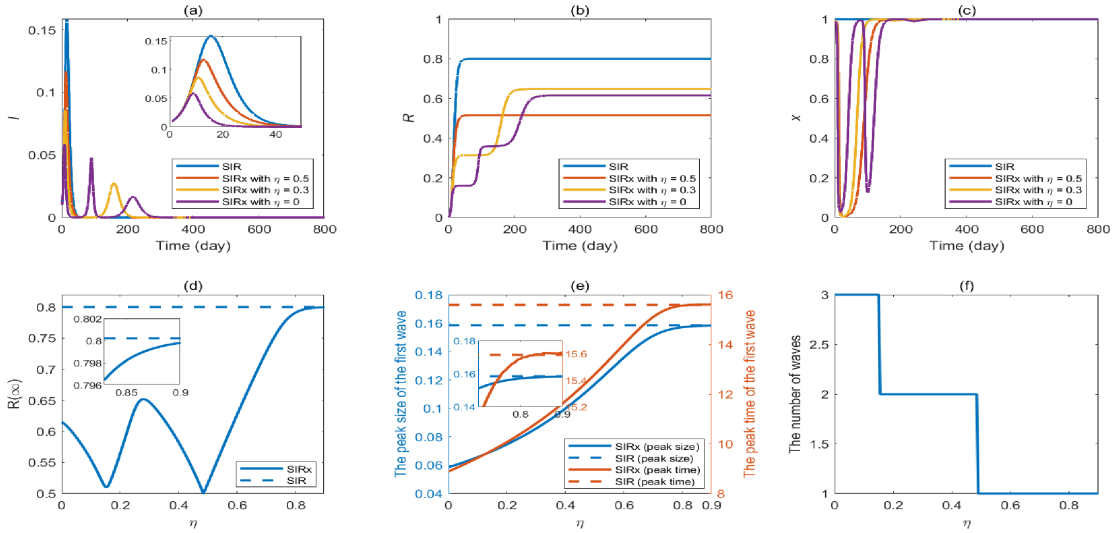

Figure 3: Numerical simulations regarding parameter η: (a)-(c) Time series of the classical SIR model and model (5.8) (denoted as "SIRx" in the figure) under different values of η. (b) Final size of the epidemic ($R(\infty)$) for model (5.8) as a function of parameter η. (e) Variation in the peak size and peak time of the first wave with parameter η. (d) Number of waves under different values of parameter η. The other parameters are fixed as follows: $\beta=0.6, \gamma=0.3, \omega=2, c=20, k=0.1$.

observed under the classic SIR model. Notably, the relationship between the final size and the parameters c, ω, η, or k is non-monotonic, as shown in Figs. 1-4(d), further emphasizing the complex interplay between behavior change and disease transmission. We also analyze the effect of the transmission rate β on behavior change, as shown in Fig. 5. The results indicate that a larger β leads to a higher peak size of the first wave and an increased number of waves. As parameter β increases, the peak time of the first wave initially increases and then decreases. Additionally, the relationship between β and the final size is non-monotonic; however, the overall trend suggests that a larger β generally results in a larger final size.

Based on the above modeling approach, Li *et al.* [40] coupled the behavioral change process, described by imitation dynamics, with the SEIS model and assumed the existence of subgroups with normal behavior (S_n, E_n) and altered behavior (S_a, E_a). Upon recovery, it was assumed that I moves back to the susceptible state, but with an altered behavior. Both births and deaths are incorporated into the model. The payoffs associated with normal and altered behaviors are modeled by

$$P_n(\tau) = -c_n I, \quad P_a(\tau) = -\widetilde{k} - c_a I$$

with $c_n > c_a$, where c_n and c_a are parameters related to the perceived risk of developing symptoms by adopting normal and altered behaviors respectively, and $\widetilde{k}$ represent the constant cost of any self-imposable prophylactic measures. The rates at which players transitioning from altered behaviors to normal behaviors or from normal behaviors to

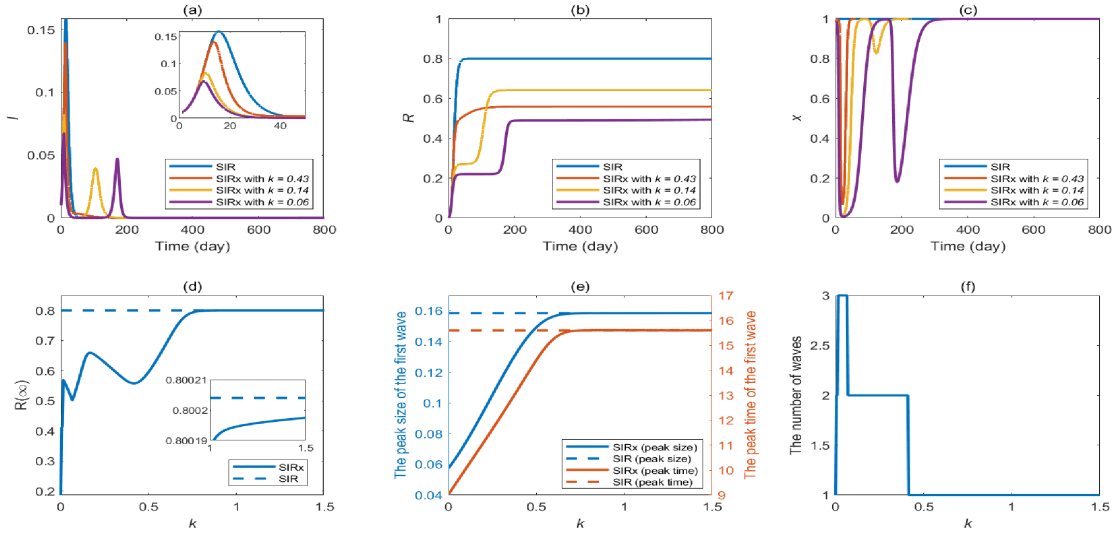

Figure 4: Numerical simulations regarding parameter k: (a)-(c) Time series of the classical SIR model and model (5.8) (denoted as "SIRx" in the figure) under different values of k. (b) Final size of the epidemic ($R(\infty)$) for model (5.8) as a function of parameter k. The dashed line represents the result under the classic SIR model. (e) Variation in the peak size and peak time of the first wave with parameter k. The dashed line represents the result under the classic SIR model. (d) Number of waves under different values of parameter k. The other parameters are fixed as follows: $\beta=0.6,\gamma=0.3,\eta=0.2,\omega=2,c=20$.

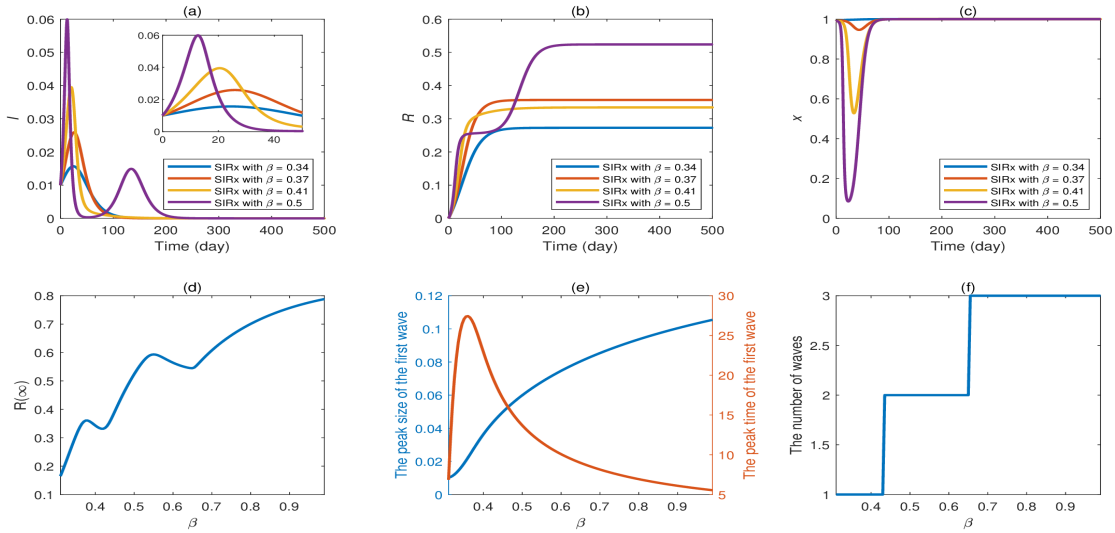

Figure 5: Numerical simulations regarding parameter β: (a)-(c) Time series of model (5.8) (denoted as "SIRx" in the figure) under different values of β. (b) Final size of the epidemic ($R(\infty)$) for model (5.8) as a function of parameter β. (e) Variation in the peak size and peak time of the first wave with parameter β. (d) Number of waves under different values of parameter β. The other parameters are fixed as follows: $\eta=0.2,\gamma=0.3,\omega=2$, $c=20,k=0.1$.

altered behaviors are defined as

$$f_{na}=\varsigma\zeta(P_n-P_a)\mathcal{H}(P_n-P_a),$$
$$f_{an}=\varsigma\zeta(P_a-P_n)\mathcal{H}(P_a-P_n),$$

respectively. Based on these assumptions, they proposed a co-evolution model that couples disease transmission dynamics with behavioral changes, incorporating the compartments S_n, S_a, E and I. By introducing the variables $S=S_n+S_a$ and $E=E_n+E_a$, they defined the variable $x=(S_n+E_n)/(S+E)$ as the fraction of the population of players adopting the normal behavior and assumed that $S_n/(S_n+S_a)=E_n/(E_n+E_a)$. Then, a model incorporating x is finally formulated

$$\begin{cases}\dot{S}(t)=\mu-[x+\eta(1-x)]\beta SI-\mu S+\gamma I,\\ \dot{E}(t)=[x+\eta(1-x)]\beta SI-\delta E-\mu E,\\ \dot{I}(t)=\delta E-\mu I-\gamma I,\\ \dot{x}(t)=-(\mu+\gamma)x\dfrac{I}{S+E}+\dfrac{\omega}{\alpha}x(1-x)(S+E)\Delta P\\ \qquad\;=-(\mu+\gamma)x\dfrac{I}{S+E}+\phi x(1-x)(S+E)(k-I),\end{cases}$$

where $\phi=(\omega/\alpha)(c_n-c_a)$ and k defines a threshold determining which behaviour is more beneficial. They demonstrated that the system undergoes a Hopf bifurcation when parameters related to behavioral change are varied. Specifically, they incorporated real behavioral data (Tokyo subway ridership) to fit and validate the model and conducted empirical analyses based on this foundation. Their findings highlighted that the interplay between behavioral changes and COVID-19 transmission is a critical factor triggering multiple waves of the pandemic. Li and Xiao [37] categorized susceptible and infectious individuals into normal and altered behavior groups. Based on the classic SIS model, they proposed two extensions: (1) a model incorporating behavior change via an imitation process, where individuals adopt the behavior with the higher payoff, and (2) a non-smooth co-evolutionary model in which the switching pattern depends solely on the fraction of individuals currently intending to change their behavior. They found that a lower prevalence threshold or a faster rate of behavior change leads to greater reductions in both daily infections and peak prevalence, along with an earlier epidemic peak in both models. However, the latter model yields a lower daily infection rate and a smaller epidemic peak compared to the former.

To better describe the perceived risk of infection, Poletti *et al.* [58] extended S_nS_aIR model by introducing infection risk as an independent compartment, M, assuming that its rate of change is positively correlated with the number of new infections. The payoffs for the two behaviors are linearly related to the infection risk M, as follows:

$$P_n=-m_nM,\quad P_a=-k-m_aM.$$

In addition to the disease transmission process within the S_n and S_a populations, they assumed that the transitions between S_n and S_a due to behavior change follow the imitation process. The transition rates f_{na} (from S_n to S_a) and f_{an} (from S_a to S_n) are directly equal to P_a and P_n, respectively. Ultimately, a coupled disease transmission and behavioral change model involving S_n, S_a, I, R, and M is obtained. Introducing the proportion of individuals adopting normal behavior, $x = S_n/S$, where $S = S_n + S_a$, the model becomes

$$\begin{cases} \dot{S}(t) = -[\beta_n S x + \beta_a S(1-x)]I, \\ \dot{I}(t) = [\beta_n S x + \beta_a S(1-x)]I - \gamma I, \\ \dot{M}(t) = [\beta_n S x + \beta_a S(1-x)]I - \theta M, \\ \dot{x}(t) = x(1-x)(\beta_a - \beta_n)I + x(1-x)[k - (m_n - m_a)M]S. \end{cases}$$

This study fitted the model using influenza data and demonstrated that individual behavioral changes can significantly impact the spread of the epidemic, altering its timeline and the scale of infections. Subsequently, Poletti *et al.* [59] further considered both symptomatic and asymptomatic infections. They assumed that the behavior of susceptible individuals, asymptomatic infected individuals, and those recovered from symptomatic infections could change behavior (either adopting altered behavior or normal behavior), and they hypothesized that the proportion of individuals adopting normal behavior is the same across these groups. The payoffs for adopting normal and altered behaviors also depend on the perceived infection risk $M(t)$, which is related to the number of new symptomatic infections. Numerical analysis was conducted to examine the impact of behavior-related parameters on the infection peak and the final size of the infection. Similarly, considering behavioral subgroups and an information variable $M(t)$ governing the signal available to individuals as a function of daily reported cases, Tang *et al.* [77] developed a co-evolutionary model for disease transmission and behavioral changes, incorporating latent individuals, asymptomatic infections, and hospitalized individuals. They fitted the model using actual COVID-19 case monitoring data and confirmed that the public's behavioral switching in response to the pandemic is a key factor triggering multiple outbreaks of COVID-19. For a comprehensive overview of research studies that use the aforementioned game theory to model individual decision-making during an epidemic, including stochastic and network-based models, refer to the review by Chang *et al.* [14].

To sum up, game theory provides a robust framework for modeling scenarios where decision-makers interact, and their choices influence one another's outcomes during a pandemic. It offers a systematic approach to predicting the behavior of rational agents in strategic situations by considering their preferences, beliefs, and possible actions. However, this modeling approach increases the dimensionality and nonlinearity of the models, thereby adding to the complexity of theoretical analysis. Moreover, it assumes that individuals are rational and consistently follow specific rules when choosing behaviors, overlooking the stochastic nature of behavioral changes in populations. Addition-

ally, studies that explore multiple strategies simultaneously using game theory remain limited. Furthermore, there is a lack of research integrating real behavioral data to validate models or conduct empirical analyses. It is important to note that other types of game theory are also applied in disease modeling. For example, vaccination behavior can be influenced by aspiration [4]. In aspiration dynamics, agents update their strategies through self-learning or self-evaluation [5]. They compare their payoff to an aspiration level to decide whether to change their behavior. Mean-field game models have been widely used to study scenarios where individuals adopt dynamic strategies, such as social distancing [17] or vaccination [21]. Mean-field game theory focuses on the strategic decision-making of small interacting agents within very large populations. By combining elements of game theory, stochastic analysis, and control theory, this framework serves as a powerful tool for understanding complex interactions in epidemiological systems.

6 Conclusion

In this review, we have primarily focused on modeling approaches for behavioral changes during disease transmission. Specifically, we categorized and reviewed articles based on three major modeling approaches: (1) revising the incidence function to incorporate behavior-driven changes, including a novel approach that describes the incidence rate using neural networks; (2) introducing additional compartments to represent subpopulations with different behaviors; and (3) employing game-theoretic modeling to analyze the interplay between infectious disease transmission dynamics and behavioral changes, including examining how the fundamental disease metrics, such as those derived from the classic SIR model, are affected when game theory is used to describe behavioral adaptations. For each category, we reviewed classical models, presented a series of extensions, and analyzed the advantages and limitations of these modeling approaches.

In the first modeling approach, it has been shown that using a non-monotonic nonlinear function to modify the incidence rate can lead to oscillations or more complex high-dimensional bifurcations in the system. When an exponential function is introduced to adjust the incidence rate, the basic reproduction number appears to remain unchanged. However, it can be demonstrated that the effect of behavioral changes may not persist throughout the entire disease period when an innovative exponential function incorporating the rate of change in cases is considered. If information levels, such as media coverage or disease-related tweets, are included, the corresponding data can be utilized to parameterize the model and improve its accuracy. Furthermore, deep learning techniques can facilitate excellent data fitting and prediction; however, they may not effectively reveal the underlying functional form of the data, such as the true incidence function. In the second modeling approach, additional compartments were introduced to represent subpopulations with different behaviors. This approach explicitly describes the evolution of behavior; however, it increases the dimensionality of the system, making theoretical analysis more challenging. By incorporating real-world surveillance data

or information-based data (such as media coverage), it can be observed that behavioral changes play a significant role in reducing disease burden. Finally, we review game-theoretic modeling of infectious disease dynamics and behavioral changes. It has been proven that the interplay between disease transmission and behavior change is a key factor contributing to the occurrence of multiple epidemic waves. Furthermore, it has been demonstrated that using game theory to predict dynamic behavioral changes is both feasible and effective. For example, this approach can accurately reproduce vaccination data [7] and subway ridership data [40]. Numerical analyses also indicate that behavioral changes influence both the peak size and the timing of the disease outbreak. In particular, we investigated the influence of modeling approaches that account for transitions between behavioral subgroups through imitation processes, within the framework of the classic SIR model, excluding birth and death rates. Our findings demonstrate that, compared to the classic SIR model without behavioral changes, incorporating behavior changes leads to a reduction in the final epidemic size. Additionally, this inclusion may lead to multiple epidemic waves while reducing the peak size of the initial wave. Importantly, the relationship between the final size and parameters associated with behavior change is non-monotonic, highlighting the intricate and complex interaction between behavioral changes and disease transmission dynamics.

These studies advance the analysis of the impact of behavior change on disease transmission. However, further exploration is warranted. For instance, incorporating age structure into the analysis could provide deeper insights, as individuals of different ages may respond to diseases differently and exhibit distinct behavioral tendencies. Then, it is possible to consider subpopulations of different age groups, assuming that the impact of behavior change on infection varies across age groups, or to further divide behavioral subgroups with transitions influenced by age structure. Additionally, most existing studies assume constant birth and death rates, neglecting the influence of external populations. To address this limitation, future research could explore patch models that account for external migration effects while minimizing the dimensionality of compartments. Furthermore, while the aforementioned modeling approaches have provided valuable insights into how individual behaviors, such as vaccination or social distancing, influence the spread of infectious diseases, they often overlook the stochastic nature of disease transmission and behavioral dynamics. Future research could utilize stochastic differential equations (SDEs) or Markov processes to more realistically capture the interactions between diseases and behavioral changes. Moreover, current studies primarily focus on population-level dynamics. Incorporating individual-level heterogeneity through network-based models could offer more comprehensive and intuitive insights into the complex interplay between behavior and disease transmission.

When disease outbreaks occur, various strategies can be implemented to mitigate transmission. However, there has been limited research utilizing game theory to examine the combined effects of pharmaceutical and non-pharmaceutical interventions on disease dynamics. Additionally, the role of delay has been largely overlooked in game-theoretic models of behavioral change. While some studies have considered delays representing

the response time for mass media to report current infections and for individuals to adapt their behaviors accordingly [70], a more systematic exploration of delay effects remains necessary. Furthermore, most existing research focuses solely on population-level behaviors. Integrating mean-field game theory to analyze both individual and collective behaviors simultaneously can provide deeper and more intuitive insights into the intricate relationship between behavior and disease transmission.

After establishing a model, fitting it to real data and conducting case studies are crucial methods for validating its effectiveness. However, when analyzing the interplay between behavior change and disease transmission, real behavioral data are rarely utilized. Although a few studies have employed public transportation data to fit models [40], extracting reliable and meaningful behavioral data and integrating it into the model remains a critical challenge. While deep learning offers a powerful approach for data fitting and prediction, it does not explicitly reveal the underlying functional form of the data Developing a deep learning-based coupled model that not only improves data fitting but also enhances model interpretability remains a challenging yet significant task.

Appendix A. The proof of Theorem 5.1

Proof. We observe that for $t>0$,

$$\frac{dS}{dt}=-[x+\eta(1-x)]\beta SI<0,$$

which implies that $\lim_{t\to\infty}S(t)=S_\infty$ exists. Similarly,

$$\frac{d(S+I)}{dt}=-\gamma I<0$$

indicates that $\lim_{t\to\infty}(S(t)+I(t))$ exists. Applying Barbalat's lemma [6], we obtain

$$\lim_{t\to\infty}\frac{d\big(S(t)+I(t)\big)}{dt}=0=-\gamma\lim_{t\to\infty}I(t),$$

leads to the conclusion that $\lim_{t\to\infty}I(t)=0$.

From Eqs. (5.8a) and (5.8b), we have

$$\frac{dI}{dS}=\frac{[x+\eta(1-x)]\beta SI-\gamma I}{-[x+\eta(1-x)]\beta SI}=-1+\frac{\gamma}{\beta}\frac{1}{S}+\frac{\gamma}{\beta}\frac{1}{S}\frac{(1-\eta)(1-x)}{x+\eta(1-x)}>-1+\frac{\gamma}{\beta}\frac{1}{S}.$$

Multiplying both sides by dS, we obtain

$$dI+dS<\frac{\gamma}{\beta}\frac{1}{S}dS.$$

Integrating both sides gives

$$I(t)+S(t)-I_0-S_0<\frac{\gamma}{\beta}\ln\left(\frac{S(t)}{S_0}\right). \tag{A.1}$$

Taking the limit as $t\to\infty$, we get

$$S_\infty-I_0-S_0<\frac{\gamma}{\beta}\ln\left(\frac{S_\infty}{S_0}\right),$$

which is equivalent to

$$\frac{\beta}{\gamma}\exp\left(S_0+I_0-\frac{\gamma}{\beta}\ln S_0\right)\geq-\frac{\beta}{\gamma}S_\infty\exp\left(-\frac{\beta}{\gamma}S_\infty\right).$$

Therefore,

$$S_\infty\geq S_\infty^{\mathrm{SIR}}=-\frac{\gamma}{\beta}LambertW\left[-\frac{\beta}{\gamma}\exp\left(-\frac{\beta}{\gamma}\left(S_0+I_0-\frac{\gamma}{\beta}\ln S_0\right)\right)\right]>0,$$

where $LambertW$ denotes the Lambert W function. Let t_* denote the time when the first peak is reached. At this moment, the condition

$$\big[x(t_*)+\eta\big(1-x(t_*)\big)\big]\beta S(t_*)=\gamma$$

holds, which implies

$$S(t_*)=\frac{\gamma}{\beta}+\frac{\gamma}{\beta}\frac{(1-\eta)\big(1-x(t_*)\big)}{x(t_*)+(1-\eta)\big(1-x(t_*)\big)}>\frac{\gamma}{\beta}.$$

Combing inequality (A.1), we obtain

$$\begin{aligned}I_{\mathrm{peak}}=I(t_*)&<I_0+S_0+\frac{\gamma}{\beta}\ln\left(\frac{S(t_*)}{S_0}\right)-S(t_*)\\&<I_0+S_0+\frac{\gamma}{\beta}\ln\left(\frac{\gamma}{\beta}\frac{1}{S_0}\right)-\frac{\gamma}{\beta}\doteq I_{\mathrm{peak}}^{\mathrm{SIR}}.\end{aligned}$$

Note that $1-S_\infty^{\mathrm{SIR}}$ and $I_{\mathrm{peak}}^{\mathrm{SIR}}$ denote the final size and peak size of the classical SIR model [13], respectively.

Sine $\lim_{t\to\infty}S(t)=S_\infty>0$ and $\lim_{t\to\infty}I(t)=0$, for any

$$0<\varepsilon<\frac{1}{2}\frac{k\omega S_\infty}{\beta+k\omega+(1-\eta)c\beta\omega S_\infty},$$

there exists $T>0$ such that for any $t>T$, we have $I(t)<\varepsilon$ and $S_\infty-\varepsilon<S(t)<S_\infty-\varepsilon$. Thus,

$$\begin{aligned}\frac{dx}{dt}&=x(1-x)\big[-\beta I+\omega S\big(k-(1-\eta)c\beta I\big)\big]\\&\geq x(1-x)\big[-\beta\varepsilon+\omega(S_\infty-\varepsilon)\big(k-(1-\eta)c\beta\varepsilon\big)\big]>0\end{aligned}$$

holds for any $t>T$. Combing with $x(t)\leq 1$, we conclude that $\lim_{t\to\infty}x(t)=1$. That completes the proof. □

Acknowledgments

The authors were supported by the National Natural Science Foundation of China (Grant No. NSFC12220101001), and by the National Key R&D Program of China (Grant No. 2022YFA1003704).

References

[1] G. Agaba, Y. Kyrychko, and K. Blyuss, *Mathematical model for the impact of awareness on the dynamics of infectious diseases*, Math. Biosci., 286:22–30, 2017.
[2] J. M. Alexander, *Evolutionary Game Theory*, Cambridge University Press, 2023.
[3] E. Aramaki, S. Maskawa, and M. Morita, *Twitter catches the flu: Detecting influenza epidemics using twitter*, in: Proceedings of the 2011 Conference on Empirical Methods in Natural Language Processing, Association for Computational Linguistics, 1568–1576, 2011.
[4] M. R. Arefin, T. Masaki, and J. Tanimoto, *Vaccinating behaviour guided by imitation and aspiration*, Proc. R. Soc. A: Math. Phys. Eng. Sci., 476:20200327, 2020.
[5] M. R. Arefin and J. Tanimoto, *Imitation and aspiration dynamics bring different evolutionary outcomes in feedback-evolving games*, Proc. R. Soc. A: Math. Phys. Eng. Sci., 477:20210240, 2021.
[6] I. Barbalat et al., *Systemes d'équations différentielles d'oscillations non linéaires*, Rev. Math. Pures Appl., 4(2):267–270, 1959.
[7] C. T. Bauch, *Imitation dynamics predict vaccinating behaviour*, Proc. R. Soc. B: Biol. Sci., 272: 1669–1675, 2005.
[8] C. T. Bauch and D. J. Earn, *Vaccination and the theory of games*, Proc. Natl. Acad. Sci. USA, 101:13391–13394, 2004.
[9] T. J. Bollyky et al., *Assessing COVID-19 pandemic policies and behaviours and their economic and educational trade-offs across US states from Jan 1, 2020, to July 31, 2022: An observational analysis*, Lancet, 401:1341–1360, 2023.
[10] M. C. Bootsma and N. M. Ferguson, *The effect of public health measures on the 1918 influenza pandemic in US cities*, Proc. Natl. Acad. Sci. USA, 104:7588–7593, 2007.
[11] S. L. Brunton and J. N. Kutz, *Data-Driven Science and Engineering: Machine Learning, Dynamical Systems, and Control*, Cambridge University Press, 2022.
[12] B. Buonomo and R. Della Marca, *Effects of information-induced behavioural changes during the COVID-19 lockdowns: The case of Italy*, R. Soc. Open Sci., 7:201635, 2020.
[13] M. Cadoni and G. Gaeta, *Size and timescale of epidemics in the SIR framework*, Phys. D, 411:132626, 2020.
[14] S. L. Chang, M. Piraveenan, P. Pattison, and M. Prokopenko, *Game theoretic modelling of infectious disease dynamics and intervention methods: A review*, J. Biol. Dyn, 14:57–89, 2020.
[15] X. Chang, J. Wang, M. Liu, Z. Jin, and D. Han, *Study on an SIHRS model of COVID-19 pandemic with impulse and time delay under media coverage*, IEEE Access, 9:49387–49397, 2021.
[16] R. T. Chen, Y. Rubanova, J. Bettencourt, and D. K. Duvenaud, *Neural ordinary differential equations*, in: Advances in Neural Information Processing Systems, Vol. 31, Curran Associates, 6571–6583, 2018.
[17] S. Cho, *Mean-field game analysis of sir model with social distancing*, arXiv:2005.06758, 2020.
[18] S. Collinson and J. M. Heffernan, *Modelling the effects of media during an influenza epidemic*, BMC Public Health , 14:376, 2014.

[19] S. Collinson, K. Khan, and J. M. Heffernan, *The effects of media reports on disease spread and important public health measurements*, PLoS One, 10:e0141423, 2015.
[20] J. Cui, Y. Sun, and H. Zhu, *The impact of media on the control of infectious diseases*, J. Dynam. Differential Equations, 20:31–53, 2008.
[21] J. Doncel, N. Gast, and B. Gaujal, *A mean field game analysis of sir dynamics with vaccination*, Probab. Engrg. Inform. Sci., 36:482–499, 2022.
[22] M. W. Fong, H. Gao, J. Y. Wong, J. Xiao, E. Y. Shiu, S. Ryu, and B. J. Cowling, *Nonpharmaceutical measures for pandemic influenza in nonhealthcare settings-social distancing measures*, Emerg. Infect. Dis., 26:976, 2020.
[23] S. Funk, E. Gilad, and V. A. Jansen, *Endemic disease, awareness, and local behavioural response*, J. Theor. Biol., 264:501–509, 2010.
[24] S. Funk, M. Salathé, and V. A. Jansen, *Modelling the influence of human behaviour on the spread of infectious diseases: A review*, J. R. Soc. Interface, 7:1247–1256, 2010.
[25] A. Glaubitz and F. Fu, *Oscillatory dynamics in the dilemma of social distancing*, Proc. R. Soc. A, 476:20200686, 2020.
[26] D. Greenhalgh, S. Rana, S. Samanta, T. Sardar, S. Bhattacharya, and J. Chattopadhyay, *Awareness programs control infectious disease – multiple delay induced mathematical model*, Appl. Math. Comput., 251:539–563, 2015.
[27] D. Helbing, I. Farkas, and T. Vicsek, *Simulating dynamical features of escape panic*, Nature, 407:487–490, 2000.
[28] D. Helbing, J. Keltsch, and P. Molnar, *Modelling the evolution of human trail systems*, Nature, 388:47–50, 1997.
[29] A. Hidano, G. Enticott, R. M. Christley, and M. C. Gates, *Modeling dynamic human behavioral changes in animal disease models: Challenges and opportunities for addressing bias*, Front. Vet. Sci., 5:137, 2018.
[30] J. Hofbauer and K. Sigmund, *Evolutionary Games and Population Dynamics*, Cambridge University Press, 1998.
[31] J. Hofbauer and K. Sigmund, *Evolutionary game dynamics*, Bull. Am. Math. Soc., 40:479–519, 2003.
[32] L. Hu and L. Nie, *Stability and Hopf bifurcation analysis of a multi-delay vector-borne disease model with presence awareness and media effect*, Fractal Fract., 7:831, 2023.
[33] I. Z. Kiss, J. Cassell, M. Recker, and P. L. Simon, *The impact of information transmission on epidemic outbreaks*, Math. Biosci., 225:1–10, 2010.
[34] A. J. Kucharski et al., *Effectiveness of isolation, testing, contact tracing, and physical distancing on reducing transmission of SARS-CoV-2 in different settings: A mathematical modelling study*, Lancet Infect Dis., 20:1151–1160, 2020.
[35] B. Kuwahara and C. T. Bauch, *Predicting Covid-19 pandemic waves with biologically and behaviorally informed universal differential equations*, Heliyon, 10(4):e25363, 2024.
[36] G. Li and Y. Dong, *Dynamic modelling of the impact of public health education on the control of emerging infectious disease*, J. Biol. Dyn., 13:502–517, 2019.
[37] L. Li and Y. Xiao, *Effect of behavior change pattern on disease transmission dynamics*, Nonlinear Dyn., 113:28579–28599, 2025.
[38] T. Li and Y. Xiao, *Linking the disease transmission to information dissemination dynamics: An insight from a multi-scale model study*, J. Theoret. Biol., 526:110796, 2021.
[39] T. Li and Y. Xiao, *Complex dynamics of an epidemic model with saturated media coverage and recovery*, Nonlinear Dyn., 107(3):2995–3023, 2022.
[40] T. Li, Y. Xiao, and J. Heffernan, *Linking spontaneous behavioral changes to disease transmission*

dynamics: Behavior change includes periodic oscillation, Bull. Math. Biol., 86(6):73, 2024.
[41] R. Liu, J. Wu, and H. Zhu, *Media/psychological impact on multiple outbreaks of emerging infectious diseases*, Comput. Math. Methods Med., 8:153–164, 2007.
[42] W.-m. Liu, H. W. Hethcote, and S. A. Levin, *Dynamical behavior of epidemiological models with nonlinear incidence rates*, J. Math. Biol., 25:359–380, 1987.
[43] W.-m. Liu, S. A. Levin, and Y. Iwasa, *Influence of nonlinear incidence rates upon the behavior of sirs epidemiological models*, J. Math. Biol., 23:187–204, 1986.
[44] Y. Liu and J.-A. Cui, *The impact of media coverage on the dynamics of infectious disease*, Int. J. Biomath., 1:65–74, 2008.
[45] M. Lu, J. Huang, S. Ruan, and P. Yu, *Bifurcation analysis of an SIRS epidemic model with a generalized nonmonotone and saturated incidence rate*, J. Differential Equations, 267:1859–1898, 2019.
[46] M. Lu, J. Huang, S. Ruan, and P. Yu, *Global dynamics of a susceptible-infectious-recovered epidemic model with a generalized nonmonotone incidence rate*, J. Dynam. Differential Equations, 33:1625–1661, 2021.
[47] P. Manfredi and A. D'Onofrio, *Modeling the Interplay Between Human Behavior and the Spread of Infectious Diseases*, Springer Science & Business Media, 2013.
[48] M. Martcheva, N. Tuncer, and C. N. Ngonghala, *Effects of social-distancing on infectious disease dynamics: An evolutionary game theory and economic perspective*, J. Biol. Dyn., 15:342–366, 2021.
[49] A. Misra, A. Sharma, and J. Li, *A mathematical model for control of vector borne diseases through media campaigns*, Discrete Contin. Dyn. Syst. Ser. B, 18(7):1909–1927, 2013.
[50] A. K. Misra, A. Sharma, and J. Shukla, *Modeling and analysis of effects of awareness programs by media on the spread of infectious diseases*, Math. Comput. Model., 53:1221–1228, 2011.
[51] L. Mitchell and J. V. Ross, *A data-driven model for influenza transmission incorporating media effects*, R. Soc. Open Sci., 3:160481, 2016.
[52] W. Msemburi, A. Karlinsky, V. Knutson, S. Aleshin-Guendel, S. Chatterji, and J. Wakefield, *The who estimates of excess mortality associated with the COVID-19 pandemic*, Nature, 613:130–137, 2023.
[53] J. Newton, *Evolutionary game theory: A renaissance*, Games, 9:31, 2018.
[54] Ş. Pamuk, *The Black Death and the origins of the 'Great Divergence' across Europe, 1300-1600*, Eur. Rev. Econ. Hist, 11:289–317, 2007.
[55] K. A. Pawelek, A. Oeldorf-Hirsch, and L. Rong, *Modeling the impact of twitter on influenza epidemics*, Math. Biosci. Eng., 11:1337–1356, 2014.
[56] S. A. Pedro, F. T. Ndjomatchoua, P. Jentsch, J. M. Tchuenche, M. Anand, and C. T. Bauch, *Conditions for a second wave of COVID-19 due to interactions between disease dynamics and social processes*, Front. Phys., 8:574514, 2020.
[57] J. Piret and G. Boivin, *Pandemics throughout history*, Front. Microbiol., 11:631736, 2021.
[58] P. Poletti, M. Ajelli, and S. Merler, *The effect of risk perception on the 2009 H1N1 pandemic influenza dynamics*, PloS One, 6:e16460, 2011.
[59] P. Poletti, M. Ajelli, and S. Merler, *Risk perception and effectiveness of uncoordinated behavioral responses in an emerging epidemic*, Math. Biosci., 238:80–89, 2012.
[60] I. Rahimi, F. Chen, and A. H. Gandomi, *A review on COVID-19 forecasting models*, Neural Comput. Appl., 35:23671–23681, 2023.
[61] R. K. Rai, S. Khajanchi, P. K. Tiwari, E. Venturino, and A. K. Misra, *Impact of social media advertisements on the transmission dynamics of COVID-19 pandemic in India*, J. Appl. Math. Comput., 68(1):19–44, 2022.
[62] S. E. Riechert and P. Hammerstein, *Game theory in the ecological context*, Annu. Rev. Ecol. Evol. Syst., 14:377–409, 1983.

[63] A. Rojas-Campos, L. Stelz, and P. Nieters, *Learning COVID-19 regional transmission using universal differential equations in a SIR model*, arXiv:2310.16804, 2023.
[64] S. Ruan and W. Wang, *Dynamical behavior of an epidemic model with a nonlinear incidence rate*, J. Differential Equations, 188:135–163, 2003.
[65] C. M. Saad-Roy and A. Traulsen, *Dynamics in a behavioral-epidemiological model for individual adherence to a nonpharmaceutical intervention*, Proc. Natl. Acad. Sci. USA, 120:e2311584120, 2023.
[66] G. P. Sahu and J. Dhar, *Dynamics of an seqihrs epidemic model with media coverage, quarantine and isolation in a community with pre-existing immunity*, J. Math. Anal. Appl., 421:1651–1672, 2015.
[67] S. Samanta, S. Rana, A. Sharma, A. K. Misra, and J. Chattopadhyay, *Effect of awareness programs by media on the epidemic outbreaks: A mathematical model*, Appl. Math. Comput., 219:6965–6977, 2013.
[68] J. M. Smith and G. R. Price, *The logic of animal conflict*, Nature, 246:15–18, 1973.
[69] P. Song and Y. Xiao, *Global Hopf bifurcation of a delayed equation describing the lag effect of media impact on the spread of infectious disease*, J. Math. Biol., 76:1249–1267, 2018.
[70] P. Song and Y. Xiao, *Analysis of an epidemic system with two response delays in media impact function*, Bull. Math. Biol., 81:1582–1612, 2019.
[71] P. Song, Y. Xiao, and J. Wu, *Discovering first principle of behavioural change in disease transmission dynamics by deep learning*, in: Mathematics of Public Health: Mathematical Modelling from the Next Generation, Springer, 37–54, 2023.
[72] J. Sooknanan and D. Comissiong, *Trending on social media: Integrating social media into infectious disease dynamics*, Bull. Math. Biol., 82:86, 2020.
[73] J. Sooknanan and T. A. Seemungal, *Fomo (fate of online media only) in infectious disease modeling: A review of compartmental models*, Int. J. Dyn. Control, 11:892–899, 2023.
[74] G. K. SteelFisher, R. J. Blendon, M. M. Bekheit, and K. Lubell, *The public's response to the 2009 H1N1 influenza pandemic*, N. Engl. J. Med., 362:e65, 2010.
[75] R. Sugden, *The Economics of Rights, Co-operation and Welfare*, Springer, 2004.
[76] C. Sun, W. Yang, J. Arino, and K. Khan, *Effect of media-induced social distancing on disease transmission in a two patch setting*, Math. Biosci., 230:87–95, 2011.
[77] B. Tang, W. Zhou, X. Wang, H. Wu, and Y. Xiao, *Controlling multiple COVID-19 epidemic waves: An insight from a multi-scale model linking the behaviour change dynamics to the disease transmission dynamics*, Bull. Math. Biol., 84:106, 2022.
[78] J. Tanimoto, *Sociophysics Approach to Epidemics*, in: Evolutionary Economics and Social Complexity Science, Vol. 23, Springer, 2021.
[79] J. M. Tchuenche and C. T. Bauch, *Dynamics of an infectious disease where media coverage influences transmission*, Int. Sch. Res. Notices, 2012:581274, 2012.
[80] J. M. Tchuenche, N. Dube, C. P. Bhunu, R. J. Smith, and C. T. Bauch, *The impact of media coverage on the transmission dynamics of human influenza*, BMC Public Health, 11:S5, 2011.
[81] P. K. Tiwari, R. K. Rai, S. Khajanchi, R. K. Gupta, and A. K. Misra, *Dynamics of coronavirus pandemic: Effects of community awareness and global information campaigns*, Eur. Phys. J. Plus, 136(10):994, 2021.
[82] F. Verelst, L. Willem, and P. Beutels, *Behavioural change models for infectious disease transmission: A systematic review (2010–2015)*, J. R. Soc. Interface, 13:20160820, 2016.
[83] J. Von Neumann and O. Morgenstern, *Theory of Games and Economic Behavior*, Princeton University Press, 1947.
[84] A. Wang and Y. Xiao, *A Filippov system describing media effects on the spread of infectious diseases*,

Nonlinear Anal.: Hybrid Syst., 11:84–97, 2014.
[85] W. Wang, *Epidemic models with nonlinear infection forces*, Math. Biosci. Eng., 3:267, 2006.
[86] Z. Wang, C. T. Bauch, S. Bhattacharyya, A. d'Onofrio, P. Manfredi, M. Perc, N. Perra, M. Salathé, and D. Zhao, *Statistical physics of vaccination*, Phys. Rep., 664:1–113, 2016.
[87] D. Weston, K. Hauck, and R. Amlôt, *Infection prevention behaviour and infectious disease modelling: A review of the literature and recommendations for the future*, BMC Public Health, 18:336, 2018.
[88] R. E. Wilson, *Mechanisms for spatio-temporal pattern formation in highway traffic models*, Philos. Trans. Roy. Soc. A, 366:2017–2032, 2008.
[89] D. Xiao and S. Ruan, *Global analysis of an epidemic model with nonmonotone incidence rate*, Math. Biosci., 208:419–429, 2007.
[90] Y. Xiao, S. Tang, and J. Wu, *Media impact switching surface during an infectious disease outbreak*, Sci. Rep., 5:7838, 2015.
[91] Y. Xiao, T. Zhao, and S. Tang, *Dynamics of an infectious diseases with media/psychology induced non-smooth incidence*, Math. Biosci. Eng., 10:445–461, 2012.
[92] Q. Yan, S. Tang, S. Gabriele, and J. Wu, *Media coverage and hospital notifications: Correlation analysis and optimal media impact duration to manage a pandemic*, J. Theoret. Biol., 390:1–13, 2016.
[93] H.-F. Zhang, Z. Yang, Z.-X. Wu, B.-H. Wang, and T. Zhou, *Braess's paradox in epidemic game: Better condition results in less payoff*, Sci. Rep., 3:3292, 2013.
[94] H. Zhao, Y. Lin, and Y. Dai, *An SIRS epidemic model incorporating media coverage with time delay*, Comput. Math. Methods Med., 2014:680743, 2014.
[95] W. Zhou, A. Wang, F. Xia, Y. Xiao, and S. Tang, *Effects of media reporting on mitigating spread of COVID-19 in the early phase of the outbreak*, Math. Biosci. Eng., 17:2693–2707, 2020.
[96] W. Zhou, Y. Xiao, and J. M. Heffernan, *Optimal media reporting intensity on mitigating spread of an emerging infectious disease*, Plos One, 14:e0213898, 2019.
[97] L. Zuo, M. Liu, and J. Wang, *The impact of awareness programs with recruitment and delay on the spread of an epidemic*, Math. Probl. Eng., 2015:235935, 2015.